Geochemistry, Geophysics, Geosystems®

RESEARCH ARTICLE
10.1029/2024GC011992

Key Points:

- The HCl and AA leaching processes dissolve the tephras and bias the extracted authigenic εNd values
- εNd of HH leachate closely matches that of foraminifera and past seawater of the Adriatic Sea
- εNd of the Adriatic Deep Water stay stable during the last 20,000 years due to vertical water mixing and local lithogenic inputs

Supporting Information:

Supporting Information may be found in the online version of this article.

Correspondence to:

C. Colin,
christophe.colin@universite-paris-saclay.fr

Citation:

Gao, G., Colin, C., Siani, G., Sepulcre, S., Pinna-Jamme, R., Haurine, F., & Dapoigny, A. (2025). Assessment of seawater Nd isotope signatures extracted from foraminiferal shells and authigenic phases from volcanogenic sediments of the Adriatic Sea. *Geochemistry, Geophysics, Geosystems*, *26*, e2024GC011992. https://doi.org/10.1029/2024GC011992

Received 31 OCT 2024
Accepted 10 FEB 2025

Author Contributions:

Data curation: Guohui Gao
Investigation: Guohui Gao, Christophe Colin
Methodology: Guohui Gao, Christophe Colin, Frederic Haurine, Arnaud Dapoigny
Writing – original draft: Guohui Gao
Writing – review & editing: Guohui Gao, Christophe Colin, Giuseppe Siani, Sophie Sepulcre, Rosella Pinna-Jamme, Frederic Haurine

Assessment of Seawater Nd Isotope Signatures Extracted From Foraminiferal Shells and Authigenic Phases From Volcanogenic Sediments of the Adriatic Sea

Guohui Gao[1], Christophe Colin[1], Giuseppe Siani[1], Sophie Sepulcre[1], Rosella Pinna-Jamme[1], Frederic Haurine[1], and Arnaud Dapoigny[2]

[1]Université Paris-Saclay, CNRS, GEOPS, Orsay, France, [2]Laboratoire des Sciences du Climat et de L'environnement, LSCE/IPSL, CEA-CNRS-UVSQ, Université Paris-Saclay, Orsay, France

Abstract The neodymium isotope signatures (εNd) of the authigenic fraction have been extensively used to reconstruct past seawater εNd and hydrological circulation. Among the various methods, sequential extraction of hydrogenic ferromanganese oxyhydroxides from bulk sediments represents a rapid and straightforward approach that may potentially induce artifacts due to the potential release of non-seawater-derived Nd during the extraction procedure. Here we investigated different methods for extracting past seawater Nd isotope compositions from a core collected in the Adriatic Sea whose tephra layers have been previously well documented. We analyzed εNd in planktonic foraminifera samples and in non-decarbonated sediment leachates obtained with three solutions commonly used in the context of the Mediterranean Sea: (a) 0.02 M hydroxylamine hydrochloride (HH) solution, (b) 1N HCl, and (b) a 25% (v/v) acetic acid (AA). Our results show that (a) the foraminiferal εNd remains unaffected by the diagenesis of tephra content; (b) all three methods indicate significantly more radiogenic εNd values in tephra levels (up to 1.5 εNd unit), which is attributed to tephra dissolution accounting for 2.7% of extracted Nd; (c) of the three leaching methods applied to samples with low tephra content, hydroxylamine hydrochloride (HH) yields εNd values that are more consistent with those obtained on planktonic foraminifera; (d) the εNd values of planktonic foraminifera in core MD90-917 remained constant indicating that the Adriatic deep water primarily reflects the local Nd isotope composition over the last 20 kyr.

Plain Language Summary Neodymium isotope signatures (εNd) from the authigenic fraction of sediments are commonly used to reconstruct past ocean circulation and seawater composition. A common method involves extracting ferromanganese oxyhydroxides from bulk sediments, which is quick and straightforward but may introduce contamination from non-seawater sources of neodymium during the process. In this study, we tested different methods for extracting εNd from a sediment core in the Adriatic Sea, known for its tephra layers, by comparing data from foraminifera and sediment leachates using three solutions: hydroxylamine hydrochloride (HH), HCl, and acetic acid (AA). We found that: (a) foraminiferal εNd is unaffected by tephra dissolution; (b) all methods showed more radiogenic εNd in tephra layers due to tephra dissolution; (c) the HH solution gave εNd values closest to foraminifera in low-tephra samples; (d) foraminiferal εNd has remained stable over the last 20,000 years, indicating Adriatic deep water reflects local neodymium isotope composition.

1. Introduction

The dissolved neodymium isotope composition ($^{143}Nd/^{144}Nd$) of seawater (expressed as εNd), has been demonstrated to be a useful proxy for tracing the provenance of water masses within the ocean (Frank, 2002; Goldstein & Jacobsen, 1987; Goldstein & Hemming, 2003; Jeandel et al., 2011; Tachikawa et al., 2003; von Blanckenburg & Igel, 1999). The residence time of Nd is relatively short, ranging from approximately 500 to 1,000 years (Siddall et al., 2008; Tachikawa et al., 1999). This is considerably less than the global turnover time of the ocean, which is estimated to be approximately 1,500 years (Broecker & Peng, 1982). Consequently, through lithogenic inputs with various Nd isotope compositions, intermediate- and deep-water masses acquire εNd from downwelling surface water. Indeed, the εNd values of water masses may be modified away from those of mixing water masses (Robinson et al., 2021; Tachikawa et al., 2017) by reversal scavenging and dissolution of particulate matter in the water column from riverine or aeolian inputs (Grenier et al., 2022; Siddall et al., 2008). Besides these "up-to-down" processes, another "bottom-up" model has also been developed. To balance the Nd isotope budget

of the ocean, it has been proposed that a process called "boundary exchange" occurs, which corresponds to the exchange of REEs between water masses and sediments deposited on the oceanic margins (Lacan & Jeandel, 2005a, 2005b; Wilson et al., 2013). In addition, recent studies have demonstrated that the benthic flux of Nd significantly modifies the Nd isotope compositions of bottom water in some oceanic regions, including the northwest Pacific Ocean (Abbott, Haley, & McManus, 2015, Abbott et al., 2019, 2019; Du et al., 2016). Moreover, tephra layers can significantly affect authigenic Nd isotope compositions in marine sediments through diagenetic processes. Volcanic materials in tephra, such as glass shards and minerals with highly radiogenic Nd isotopic compositions, can dissolve and release Nd into pore waters and bottom waters, altering the authigenic signal intended to reflect past seawater composition (Gieskes et al., 1990; Spivack & Staudigel, 1994; Pichler et al., 1999; Morin et al., 2015). These processes highlight the non-conservative characteristic of Nd isotopes, a factor which should be considered when applying εNd proxies to reconstruct past hydrological conditions of water masses. However, in areas far from the continental margins and regions associated with strong benthic flux, the only way to alter the initial isotopic composition of a water mass is for it to mix with other water masses characterized by different isotopic compositions. Consequently, εNd can be considered as a quasi-conservative tracer.

In the Mediterranean Sea, the seawater εNd values display a large range from -11 to -5. Atlantic surface water (AW) is characterized by unradiogenic εNd (-11), which contrasts strongly with the radiogenic intermediate and deep waters from the Levantine basin (-5). The latter have acquired radiogenic isotopic composition through water exchanges with the particularly high radiogenic sediments of volcanic origin on the southern and eastern margins of the Levantine basin (Henry et al., 1994; Montagna et al., 2022; Tachikawa et al., 2004; Vance et al., 2004). The distribution of seawater εNd values exhibits a distinct correlation with salinity, with contrasted differences in εNd signatures observed between the different surface, intermediate, and deep-water masses. This reflects the large-scale basin circulation of the Mediterranean Sea (Montagna et al., 2022).

Although some questions regarding the Nd budget of the Mediterranean Sea, including the role of boundary exchange, benthic flux, and biological cycling still remain, the εNd proxy has been used over the past decade to reconstruct past circulation changes at different time scales in the Mediterranean Sea (Colin et al., 2021; Cornuault et al., 2018; Dubois-Dauphin et al., 2017; Duhamel et al., 2020; Jiménez-Espejo et al., 2015; Osborne et al., 2010; Wu et al., 2019). Past εNd of water masses in the Mediterranean Sea have been extracted using several analytical procedures, many of which remain a subject of debate within the scientific community. Nd isotope compositions have been obtained from fish debris/teeth (Wu et al., 2019), planktonic foraminifera (Colin et al., 2021; Cornuault et al., 2018; Duhamel et al., 2020; Jiménez-Espejo et al., 2015; Osborne et al., 2010; Scrivner et al., 2004; Vance et al., 2004; Wu et al., 2019), cold-water corals (Dubois-Dauphin et al., 2017) and authigenic oxy-hydroxides, using various analytical procedures such as bulk sediment leached with 1 M HCl (Freydier et al., 2001; Wu et al., 2019) and hydroxylamine hydrochloride leaching of non-decarbonated samples (Cornuault et al., 2018; Tachikawa et al., 2004).

Each method has inherent advantages and inconveniences, and the results may be affected by potential bias mainly due to contamination from lithogenic Nd of the detrital fraction (e.g., Wilson et al., 2013) or early diagenetic overprinting (e.g., Skinner et al., 2019). Ideally, foraminifera or fish fragments should be hand-picked from marine sediments in order to reconstruct the most reliable and continuous deep-water Nd isotope signatures over time scales of thousands of years. However, foraminifera and fish teeth fragments are often not available in sufficient quantities, particularly in the Mediterranean Sea, to carry out consistent studies for the reconstruction of seawater εNd at high temporal resolutions. Similarly, although deep-sea corals allow for strong age control and high temporal resolution, they mainly thrive at mid-depths, rendering continuous temporal coral-based coverage unachievable. To overcome these shortcomings, alternative archives should be considered. In this regard, the extraction of deep seawater-derived Nd from hydrogenic Fe-Mn oxyhydroxides of bulk sediments represents a highly advantageous approach, as it can be applied to a large variety of sediments (not constrained by the abundance of foraminifera or fish debris) and is much less time-consuming. In their studies, Wilson et al. (2013) and Blaser et al. (2016) have reassessed the reliability of different approaches for extracting Nd isotopes preserved in Fe-Mn coatings. They propose that short leaching times and high sediment/solution ratios permit the extraction of seawater εNd from sediments and could be considered as a reliable method for reconstructing past seawater εNd. Nevertheless, it is essential to evaluate the analytical procedure on a case-by-case basis rather than applying it as a standardized method across all sites.

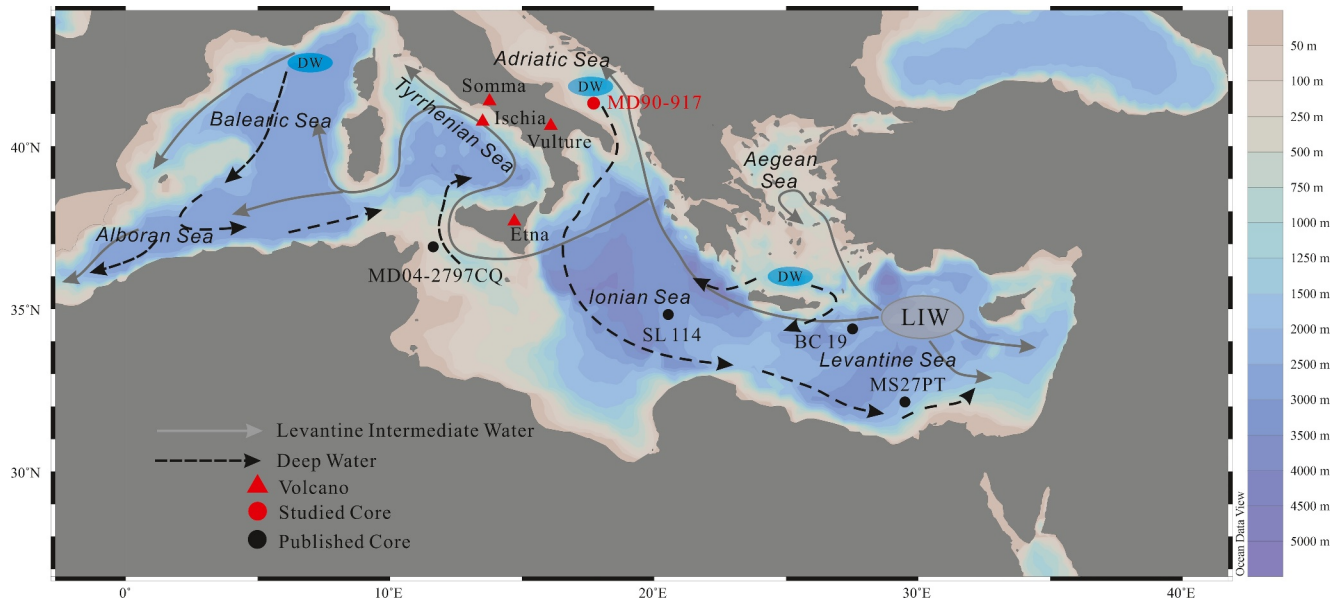

Figure 1. Bathymetric map of the Mediterranean Sea showing the location of core MD90-917 (41°17N; 17°378E; 1,010 m water depth). The simplified modern Mediterranean water circulation is broadly indicated (Rogerson et al., 2012; Rohling et al., 2015). The dashed dark line represents the deep-water circulation, while the solid gray line depicts the intermediate water circulation. The red triangles indicate the locations of volcanoes in Italy. The map was generated using Ocean Data View software. Location of cores MS27PT, MD04-2797CQ, SL114 and BC19 discussed in this study have also been reported.

The central part of the Mediterranean Sea is a key area for reconstructing past water mass exchange; it has been characterized by contrasted εNd values between the Eastern and Western Mediterranean basins, with the Siculo-Tunisian Strait acting as a conduit for this exchange. Additionally, the relative contributions through time of the Adriatic Sea and Aegean Sea to the production of deep-water masses in the Eastern basin is a topic of interest, with studies such as those conducted by Cornuault et al. (2018) and Colin et al. (2021) contributing to our understanding of this process. Furthermore, the central part of the Mediterranean Sea is affected by the deposition of abundant ash layers (Ayuso et al., 1998; D'Antonio et al., 2007; Siani et al., 2004), which have the potential to alter the Nd isotope composition by the easy dissolution of volcanic glass during the diagenesis process or during the sequential extraction of authigenic Fe-Mn oxy-hydroxides (Crovisier et al., 1987; Kent et al., 1999; Schacht et al., 2008).

The central-southern Adriatic Sea is an ideal region for the preservation of tephra layers allowing detailed tephrochronological studies (Bourne et al., 2010; Calanchi & Dinelli, 2008; Matthews et al., 2015; Paterne et al., 1988; Siani et al., 2004; Totaro et al., 2022) due to the fact that it is currently downwind of Italian volcanic sources (i.e., Somma-Vesuvius, Campi Flegrei, Mt. Etna, Ischia and Lipari islands) that were active during the Quaternary and show a high sedimentation rate of the sedimentary sequence.

In this study, we extracted seawater Nd isotope composition (εNd) from planktonic foraminifera and authigenic ferromanganese oxyhydroxides using three different analytical procedures previously used in the Mediterranean Sea (non-decarbonated sediment leached with HCl, acetic acid and hydroxylamine hydrochloride); our focus is a core from the South Adriatic Sea where 14 tephra layers have been previously well determined (Siani et al., 2004). The objective was to evaluate how the diagenesis and dissolution of volcanic tephra impacts the Nd isotope composition of the authigenic Fe–Mn oxyhydroxide phases. Furthermore, the study aims to determine how detrital and volcanic materials may have modified the εNd signal extracted using the three different analytical methods.

2. Materials and Methods

2.1. Sediment Samples

Core MD90-917 was collected during the PROMETE II expedition in 1990 by the French *R/V Marion Dufresne* in the South Adriatic deep basin (41°17N; 17°378E; 1,010 m water depth, Figure 1). The lithology of the core

consists of 21 m of gray to brown carbonaceous clays, including a black layer in the upper part of the core between 229 and 257 cm, referred to as the S1 sapropel. The sapropel S1 deposition is divided in two by a thin horizon of white hemipelagic ooze between 239 and 247 cm. The relative abundance of glass shards was assessed by Siani et al. (2004) and allowed the identification of 14 ash layers. In the present study, 21 samples were selected in the first 7 m of the core. Of these samples, 11 were collected from the tephra layer and an additional 10 samples were collected from sediments devoid of ashes. The objective was to investigate the influence of tephra on authigenic Nd isotope compositions extracted from the samples using a different analytical method.

The age model of the core has been established by Siani et al. (2004, 2010). ^{14}C dating was performed on monospecific planktonic foraminifera in the more than 150 μm size fraction and was corrected to a surface marine ^{14}C reservoir age of 400 years, except for the early deglaciation, where this value is doubled (Siani et al., 2000, 2001). The presence of 14 ash layers identified along the first 7 m of the core allowed the chronology to be refined (Siani et al., 2004). Here, we provide an updated version of the previous age model, which has been revised using the calibration based on IntCal20 (Reimer et al., 2020). The mean sedimentation rate of the studied interval is approximately 40 cm.kyr^{-1} which allows us for the first time to establish a high temporal resolution of the εNd record of the last 20 cal kyr for the deep water of the Adriatic Sea.

2.2. Methods

2.2.1. REE Concentration Analyses

Rare Earth Element (REE) concentrations were analyzed using a single collector sector field high resolution inductively coupled plasma mass spectrometer (HR-ICP-MS) Thermo Element XR at PANOPLY's analytical facilities hosted at the *Laboratoire Géosciences Paris-Saclay* (*GEOPS*), the *University Paris-Saclay*, France. REE concentrations were calculated using the uFREASI software (Tharaud et al., 2015). All samples were analyzed at a Ca concentration of 5 ppm in order to avoid significant matrix effects. The accuracy of the determination of REE concentrations was validated by analysis of two geological standards, BCR-2 and BHVO2, prepared at various dilutions with offsets systematically lower than 5%. Blank contributions are considered negligible for all REEs since analysis of chemical blanks (spike solutions before and after chemistry) revealed a REE signal systematically lower than 1% (most often less than 1‰) compared to REE signals measured for each sample. Finally, our measurements were characterized by analytical uncertainties that were systematically below 10% (2σ) for all REEs.

REEs were normalized to Post Archean Australian Shale (PAAS, Nance & Taylor, 1976) to evaluate the REE pattern. The following parameters were used (all PAAS normalized values, after Martin et al., 2010): LREE = La + Pr + Nd, MREE = Gd + Tb + Dy, HREE = Tm + Yb + Lu, MREE/MREE* = 2xMREE/(LREE + HREE), Ce/Ce* = 2xCe/(La + Pr).

2.2.2. Nd Isotope Composition Analyses

Nd isotope composition analyses were carried out on the siliciclastic fraction, planktonic foraminifera samples and on leachate of authigenic ferromanganese oxyhydroxides using different leaching procedures, namely 0.02 M hydroxylamine hydrochloride (HH) solution, 1N HCl, and a 25% (v/v) acetic acid (AA).

Nd isotope compositions were firstly analyzed on the siliciclastic fraction of core MD90-917. Sediment samples were then treated with acetic acid (25%) and hydrogen peroxide (33%) to remove carbonate and organic matter, respectively.

Nd isotope compositions were also analyzed on ∼30 mg mixed planktonic foraminifera from the >150 μm size fraction, with no oxidative-reductive cleaning procedure, as this approach has been demonstrated to be suitable for extracting deep-water Nd isotope compositions (e.g., Tachikawa et al., 2014; Wu et al., 2015). The foraminifera samples were gently crushed between two glass slides under the microscope to open all chambers, and then ultrasonicated for 1 min in *MilliQ* water before pipetting off the suspended particles. This step was repeated until the water was clear and free of clay particles. The remaining foraminifera were dissolved using weak leaching with stepwise 100 μl nitric acid (0.5 M HNO_3). The dissolved samples were centrifuged and the supernatant was immediately transferred to Teflon beakers to prevent leaching of any possible remaining solid phases.

Several studies have been carried out to test the reliability of seawater-derived Nd extraction from bulk sediments involving different leaching procedures (Bayon et al., 2002; Gutjahr et al., 2007; Wilson et al., 2013). In accordance with Wilson et al. (2013) and Blaser et al. (2016), no removal of the carbonate fraction of the bulk sediments was performed, and short leaching times and large sample size/leachate ratios were adopted for our sample processing. In this study, a sequential analysis was then carried out on ground samples of 1 g, which were simply rinsed with deionized water and then directly leached with 7 ml 0.02 M hydroxylamine hydrochloride (HH solution) for 2 min. In addition, two sets of 100 mg of bulk sediments were leached with 10 ml of 1N HCl and 25% (v/v) acetic acid (AA), respectively, for 30 min. For the three analytical procedures, the extracted leachate was ultra-centrifugated and the supernatant was transferred to Teflon beakers and dried on a hot plate before the Nd purification step.

Neodymium was then separated following the analytical procedure described by Copard et al. (2010). Briefly, samples were loaded in 2 ml of 1 M HNO_3 into pre-conditioned columns (with 83 mg of TRUspec™ resin). Unwanted cations were eluted using five portions of 0.5 ml of 1 M HNO_3. The TRUspec™ columns were then placed over the LNspec™ columns. The light REEs were eluted from the upper columns to the LNspec™ columns using seven portions of 0.05 M HNO_3. After decoupling from the TRUspec™ columns, La, Ce, and most of the Pr were rinsed from the LNspec™ columns with 2.5 ml of 0.25 M HCl. Neodymium was then eluted with an additional 3.25 ml of 0.25 M HCl.

The $^{143}Nd/^{144}Nd$ ratios of purified Nd fractions were measured by Multi-Collector Inductively Coupled Plasma Mass Spectrometry (MC-ICP-MS, *Thermo Fisher Neptune^{Plus}*) at PANOPLY's analytical facilities hosted at the *Laboratoire des Sciences du Climat et de l'Environnement* (*LSCE*, France) at the *University Paris-Saclay*, France. The solutions were analyzed at a concentration of 10–15 ppb. The mass-fractionation correction was made by normalizing $^{146}Nd/^{144}Nd$ to 0.7219 (O'Nions et al., 1977), applying the exponential-fractionation law. During the analysis, every group of three samples was bracketed with the JNdi-1 standard with Nd concentrations similar to those of the samples. Replicate analyses of the JNdi-1 standards yielded mean $^{143}Nd/^{144}Nd$ ratios of 0.512108 ± 0.000009 (2σ, n = 32), closely matching the accepted value of 0.512115 ± 0.000006 (Tanaka et al., 2000). The external reproducibility (2s) of the εNd values obtained from repeated measurements of the JNdi-1 standard ranged from 0.2 to 0.4 εNd units for the different analytical sessions. The reported analytical uncertainty is a combination of the external reproducibility of the within-session standards and the internal measurement error of each sample. Total blanks were <30 pg and can be ignored as they represent <0.1% of the sample characterized by the lowest amount of Nd. Neodymium isotope compositions are expressed as $\varepsilon Nd = [(^{143}Nd/^{144}Nd)_{sample}/(^{143}Nd/^{144}Nd)_{CHUR}-1] \times 10{,}000$, with the present-day $(^{143}Nd/^{144}Nd)_{CHUR}$ of 0.512638 (Jacobsen & Wasserburg, 1980).

3. Results

3.1. REE Concentrations

The PAAS-normalized REE patterns exhibit enrichment of MREE with MREE* values exceeding 1.5 for all samples obtained from the three leaching procedures, regardless of the presence or absence of tephra (Table 1 and Figure 2). In general, the transition from LREE to MREE is less pronounced in samples containing tephra compared to samples without tephra, while the REE concentrations are slightly higher for samples in tephra layers for all three leaching methods (Figure 2).

The HREE/LREE ratios vary from 0.79 to 1.29. Overall, samples with high volcanic ash content exhibit ratios below 1 suggesting relative enrichment of LREE, whereas other samples have ratios above 1 indicating HREE enrichment (Table 1). The Ce* values of the three leaching methods show variation but remain consistently below 1, indicating a negative anomaly (Table 1, Figure 2).

3.2. εNd of Foraminifera, Bulk Sediment Leaching, and Detrital Fraction

The εNd values of the foraminifera show a narrow range from −6.46 ± 0.27 to −5.85 ± 0.36 (Table 3, Figure 3a). Conversely, the εNd values obtained by the three leaching methods display large variations, with HCl leaching yielding values between −4.51 ± 0.31 and −7.29 ± 0.25, AA leaching yielding values between −5.12 ± 0.12 and −7.09 ± 0.31, and HH leaching yielding values between −5.00 ± 0.13 and −6.95 ± 0.2. The detrital material shows a more unradiogenic range of εNd values, varying from −5.14 ± 0.13 to −9.61 ± 0.14 (Table 2).

Table 1
Rare Earth Element Results of Leachate Obtained for 1 N HCl Leachate, 25% Acetic Acid Leachate and 0.02 M Hydroxylamine Hydrochloride (HH) Leachate From Samples Collected in Core MD90-917

				0.02 M hydroxylamine hydrochloride (HH) leachate			1N HCl leachate			25% (v/v) acetic acid (AA) leachate		
Depth (cm)	Age (yr)	Carbonate content %	Tephra content %	Ce*	HREE/LREE	MREE*	Ce*	HREE/LREE	MREE*	Ce*	HREE/LREE	MREE*
18	939	27.9	3.3	1.01	1.22	1.65	0.90	1.14	1.63	0.92	1.14	1.67
75	2,423	25.4	2.7	0.96	1.27	1.55	0.98	1.14	1.63	0.95	1.00	1.87
133.5	4,046	28.2	20.6	0.95	0.95	1.71	0.93	0.88	1.78	0.90	0.93	1.74
152.5	4,554	27.5	66.8	0.92	0.97	1.64	0.95	0.78	1.82	0.90	0.82	1.75
167.5	5,018	24.1	65.4	0.86	0.94	1.59	0.92	0.75	1.71	0.91	0.84	1.64
205	6,510	12.7	5.4	0.89	1.20	1.88	0.93	1.15	1.90	0.93	1.13	1.83
237.5	8,097	27.8	9.1	0.90	0.97	1.70	0.94	1.05	1.74	0.89	1.02	1.78
252.5	8,739	27.3	25.4	0.88	1.35	1.69	0.93	0.99	1.97	0.89	1.09	1.91
285	11,861	31.6	1.5	0.93	0.99	1.77	0.89	0.94	1.89	0.86	1.03	1.77
305.5	12,316	17.5	67.0	0.89	0.89	1.53	0.94	0.69	1.65	0.92	0.74	1.69
365	13,486	30.4	1.6	0.90	1.08	1.78	0.94	0.92	2.00	0.93	1.02	1.87
393.5	13,945	24.1	84.9	0.92	0.90	1.60	0.91	0.81	1.56	0.91	0.79	1.62
410.5	14,928	23.8	69.7	0.89	0.89	1.50	0.94	0.82	1.68	0.91	0.88	1.53
430	15,319	24.3	2.4	0.94	1.15	1.63	0.92	0.94	1.84	0.92	0.89	1.81
460	16,086	37.6	1.8	0.90	1.24	1.64	0.90	0.95	1.91	0.95	1.04	1.80
510	17,831	31.2	0.6	0.91	1.18	1.82	0.88	1.00	2.01	0.88	1.09	1.82
530.5	18,945	11.4	16.3	0.88	0.78	1.41	0.89	0.54	1.33	0.92	0.87	1.54
575	20,468	30.0	0.8	0.89	1.07	1.88	0.89	1.06	1.84	0.95	1.09	1.82
635	21,413	33.9	6.0	0.90	1.09	1.68	0.83	0.97	1.77	0.89	1.01	1.79
665	22,350	21.3	2.3	0.88	1.16	1.79	0.88	1.07	1.85	0.86	1.09	1.83
701	23,444	23.1	6.6	0.89	1.08	1.59	0.85	1.00	1.77	0.89	1.00	1.87

Note. LREE = La + Pr + Nd, MREE = Gd + Tb + Dy, HREE = Tm + Yb + Lu, MREE/MREE* = 2xMREE/(LREE + HREE), Ce/Ce* = 2xCe/(La + Pr).

The εNd values obtained with the three leaching methods and the carbonate-free fraction on the same sediment are more radiogenic as the tephra content increases (Table 2 and Figure 3). On the contrary, the εNd values obtained from the foraminiferal samples are not modified by the presence of tephra and remain constant throughout the core (Figure 3a). However, foraminiferal εNd values are consistently more negative than those obtained for the three leachates for samples within tephra layers, whereas they are more radiogenic for samples outside tephra layers (Figure 3 and Table 2). Of the three leaching methods, HH-leaches display εNd values closest to those of the foraminiferal samples, although there is a slight offset. This offset is definitively more important when using AA-leaches. The HCl-leaches show the greatest divergence from foraminiferal εNd (Figure 3b).

Positive correlations between tephra contents and leachate εNd are observed for samples located within tephra layers (r^2 = 0.22 for HH-leaches, 0.33 for AA-leaches and 0.34 for HCl-leaches), where εNd becomes more radiogenic with higher tephra contents (Figures 4a, 4c, and 4e). However, tephra contents and Nd concentrations do not show any correlation for these samples (Figures 4a, 4c, and 4e). On the contrary, samples collected outside the tephra layers showed no significant correlations between tephra contents versus either εNd values or Nd concentrations (Figures 4b, 4d, and 4f). On the other hand, an evident correlation was observed between leachate εNd versus carbonate content (r^2 = 0.55 for HH-leaches, 0.32 for AA-leaches and 0.29 for HCl-leaches) and between Nd concentrations versus carbonate content (r^2 = 0.64 for HH-leaches, 0.72 for AA-leaches and 0.69 for HCl-leaches) (Figures 5a, 5c, and 5e). In general, for samples taken from tephra layers, εNd exhibits a trend toward more radiogenic values while Nd concentration increases with decreasing carbonate content. However, no significant relationships between carbonate contents and εNd or Nd concentrations can be observed for samples collected outside the tephra layers (Figures 5b, 5d, and 5f).

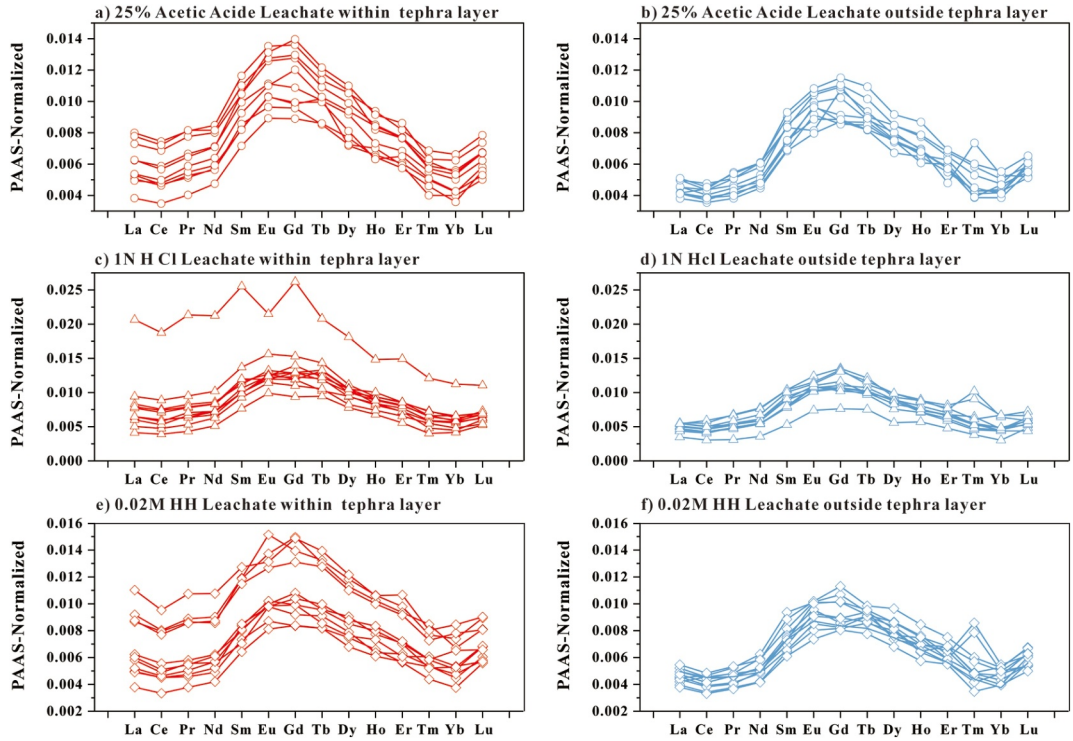

Figure 2. PAAS-normalized Rare Earth Element patterns obtained on 25% Acetic Acid leachate, 1N HCl leachate, and 0.02M hydroxylamine hydrochloride (HH) leachate from samples collected in tephra layers (red curves, a, c and e) and non-tephra layers (blue curves, b, d and f).

4. Discussion

Tachikawa et al. (2014) have shown that the Nd-rich phases associated with foraminifera mainly consist of Fe-Mn oxides adhered to calcite surfaces, and Fe oxide/oxyhydroxide phases found within the pores and internal chambers of foraminifera. The Fe-Mn coating predominantly records the signal from bottom water conditions and/or pore water (Piepgras & Wasserburg, 1987; Roberts et al., 2010; Stoll et al., 2007; Tachikawa et al., 2014).

Core-top samples of foraminifera from core MD90-917 have an εNd value (-6.10 ± 0.35; Figure 3a) that is slightly more radiogenic than modern deep-water from nearby stations (εNd between -7.57 ± 0.50 and -7.31 ± 0.50, St. Arcadia, St. 64PE374-8 and St. 64PE374-9; Montagna et al., 2022). The εNd values recorded for the three weak acid-leaches (-6.79 ± 0.16 for HH-leaches, -6.95 ± 0.25 for HCl-leaches, and -6.59 ± 0.25 for AA-leaches, Figure 3b) display a slight negative offset compared to the foraminiferal εNd value (Figure 3b).

Authigenic εNd can be influenced by processes occurring during early diagenesis (e.g., Elderfield et al., 1981; Elderfield & Sholkovitz, 1987; Grousset et al., 1988). This could therefore be partly due to remobilization of Nd from authigenic and lithogenic fractions during diagenesis (Bayon et al., 2004). The detrital fraction of core MD90-917 shows a large range of εNd values between the tephra (mean of about -5) and non-tephra layers (mean of about -9) (Table 2 and Figure 3a). This implies that the εNd values of the detrital fraction result from the mixing of unradiogenic crustal material deriving mainly from the surrounding small rivers and the major Po River (εNd of -11, Malusà et al., 2017; Weldeab et al., 2002) and from radiogenic volcanic material (from -1.0 ± 0.1 to $+3.2 \pm 0.2$, D'Antonio et al., 2016).

4.1. Potential Role of Tephra in Authigenic Fe-Mn

The analytical procedure of sediment-leaching has great potential to provide extensive spatial coverage and high temporal resolution, especially in marine sediments where the amount of foraminifera is insufficient for Nd isotope composition analyses (Crocket et al., 2011; Piotrowski et al., 2004, 2008; Rutberg et al., 2000), such as the low carbonate content of the tephra layers of core MD90-917 (Table 1).

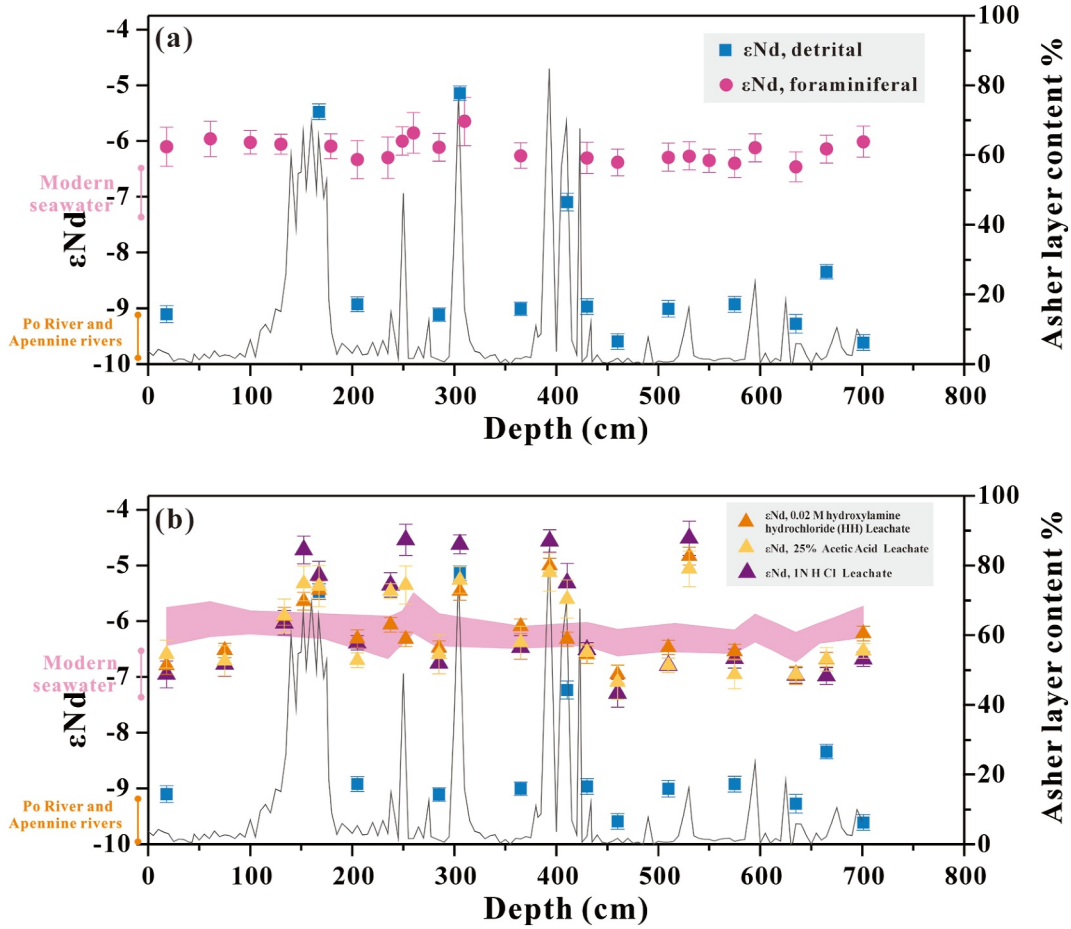

Figure 3. (a) Variations of the εNd obtained on mixed planktonic foraminifera (pink circles) and carbonate-free fraction (blue squares) along with the content of the tephra layer; (b) variations of the εNd obtained acid leachate (yellow and purple triangles) and 0.02 M hydroxylamine hydrochloride (HH) (orange triangles) with the content of the tephra layer for core MD90-917; the pink bar is the signature of foraminiferal εNd (MD90-917). The modern AeDW εNd have also been reported for the south Adriatic Sea and the Northern Ionian Sea (Garcia-Solsona et al., 2020; Montagna et al., 2022). The detrital sediment εNd of Po River is from (Malusà et al., 2017) and Apennine River is from (Weldeab et al., 2002). We have also reported (dark line) the relative abundance of glass shards by Siani et al. (2004), which allows us to identify several ash layers.

The distinctive normalized-REE patterns obtained in leachates can provide information on the specific extracted phase, as different phases exhibit their own characteristic REE patterns (Gutjahr et al., 2007; Palmer, 1985; Palmer & Elderfield, 1986; Pattan & Parthiban, 2007; Piotrowski et al., 2012; Shields & Webb, 2004; Tachikawa et al., 2013). The normalized-REE pattern of the leachates without tephra has been compared to that of seawater, which exhibits a negative Ce anomaly and enrichment in HREE (Bau et al., 1997; Censi et al., 2007), the ash layer (which exhibits LREE enrichment, Ayuso et al., 1998), the detrital component (which exhibits a flat normalized-REE pattern, Wu et al., 2018), the planktonic foraminifera (which exhibit MREE enrichment, Halay et al., 2004) and the ferromanganese nodules (which exhibit MREE enrichment, Pattan & Parthiban, 2007) (Figure S1 in Supporting Information S1). The samples from all three leaching methods, within or outside a tephra-layer, exhibit a significant MREE enrichment pattern suggesting that Fe-Mn coatings are the primary phase present in the extracted leachate (Figure 2). However, the samples located in the tephra layers exhibit a slight enrichment in LREE compared to non-tephra layers, suggesting that the tephra could also be extracted during the leaching process (Table 1). These findings are consistent with the correlation trend observed between leachate εNd and tephra contents, whereby more radiogenic εNd values are associated with a greater proportion of tephra (Figures 4 and 5). This confirms the hypothesis that a detrital radiogenic volcanic component can also modify the Nd isotope signature of leachates (Elmore et al., 2011; Roberts et al., 2010; Vance et al., 2004).

Geochemistry, Geophysics, Geosystems

10.1029/2024GC011992

Table 2

Nd Isotope Compositions and Concentrations Obtained for 1 N HCl Leachate, 25% Acetic Acid Leachate and 0.02 M Hydroxylamine Hydrochloride (HH) Leachate From Samples Collected in Core MD90-917

		0.02 M hydroxylamine hydrochloride (HH) leachate					1 N HCl leachate					25% acetic acid leachate					Detrital			
Depth (cm)	Age (yrs)	$^{143}Nd/^{144}Nd$	±2sigma	εNd	±2sigma	[Nd] ppm	$^{143}Nd/^{144}Nd$	±2sigma	εNd	±2sigma	[Nd] ppm	$^{143}Nd/^{144}Nd$	±2sigma	εNd	±2sigma	[Nd] ppm	$^{143}Nd/^{144}Nd$	±2sigma	εNd	±2sigma
18	939	0.512290	0.000008	−6.79	0.16	2.01	0.512282	0.000013	−6.95	0.24	2.63	0.512300	0.000013	−6.59	0.25	2.07	0.512172	0.000008	−9.10	0.15
75	2,423	0.512304	0.000007	−6.52	0.13	2.12	0.512291	0.000011	−6.77	0.22	2.59	0.512294	0.000014	−6.71	0.27	1.8				
133.5	4,046	0.512335	0.000008	−5.91	0.16	1.66	0.512329	0.000011	−6.03	0.22	2.44	0.512335	0.000015	−5.9	0.3	1.94				
152.5	4,554	0.512349	0.000008	−5.64	0.16	2.11	0.512396	0.000013	−4.72	0.25	2.29	0.512365	0.000016	−5.32	0.31	1.91				
167.5	5,018	0.512359	0.000008	−5.44	0.16	1.9	0.512372	0.000013	−5.18	0.26	2.82	0.512363	0.000019	−5.37	0.37	2.42	0.512357	0.000007	−5.47	0.14
205	6,510	0.512315	0.000008	−6.31	0.16	1.42	0.512310	0.000007	−6.39	0.13	1.21	0.512310	0.000007	−6.7	0.13	1.51	0.512181	0.000007	−8.92	0.13
237.5	8,097	0.512327	0.000007	−6.06	0.13	1.71	0.512364	0.000011	−5.35	0.22	1.98	0.512358	0.000015	−5.46	0.13	1.65				
252.5	8,739	0.512314	0.000007	−6.32	0.13	1.42	0.512405	0.000015	−4.54	0.28	1.74	0.512364	0.000017	−5.35	0.34	1.61				
285	11,861	0.512306	0.000007	−6.48	0.13	1.76	0.512292	0.000010	−6.75	0.19	2.08	0.512300	0.000018	−6.59	0.35	1.97	0.512171	0.000006	−9.11	0.12
305.5	12,316	0.512358	0.000008	−5.46	0.16	3.06	0.512401	0.000009	−4.62	0.17	3.45	0.512368	0.000012	−5.26	0.24	2.87	0.512375	0.000007	−5.14	0.13
365	13,486	0.512326	0.000007	−6.09	0.13	1.98	0.512306	0.000011	−6.47	0.21	1.83	0.512311	0.000015	−6.38	0.29	1.57	0.512177	0.000006	−9	0.12
393.5	13,945	0.512382	0.000007	−5	0.13	2.91	0.512404	0.000010	−4.56	0.2	2.92	0.512375	0.000017	−5.12	0.34	2.71				
410.5	14,928	0.512314	0.000007	−6.32	0.13	2.96	0.512366	0.000018	−5.31	0.35	2.83	0.512351	0.000018	−5.6	0.34	2.77	0.512267	0.000008	−7.23	0.16
430	15,319	0.512299	0.000008	−6.6	0.16	1.77	0.512304	0.000007	−6.51	0.13	2.13	0.512302	0.000007	−6.55	0.13	2.01	0.512179	0.000007	−8.96	0.14
460	16,086	0.512282	0.000008	−6.95	0.16	1.64	0.512264	0.000013	−7.29	0.25	2.08	0.512274	0.000016	−7.09	0.31	2.07	0.512147	0.000007	−9.59	0.14
510	17,831	0.512306	0.000007	−6.47	0.13	1.67	0.512290	0.000007	−6.79	0.13	1.87	0.512290	0.000007	−6.79	0.13	1.72	0.512177	0.000008	−9	0.15
530.5	18,945	0.512390	0.000008	−4.83	0.16	3.65	0.512407	0.000016	−4.51	0.31	7.2	0.512378	0.000016	−5.06	0.32	4				
575	20,468	0.512303	0.000007	−6.54	0.13	1.41	0.512296	0.000009	−6.67	0.17	1.84	0.512282	0.000013	−6.95	0.26	1.62	0.512181	0.000007	−8.92	0.14
635	21,413	0.512281	0.000008	−6.97	0.16	1.93	0.512281	0.000007	−6.97	0.14	2.47	0.512282	0.000007	−6.95	0.13	2.16	0.512163	0.000009	−9.27	0.17
665	22,350	0.512295	0.000007	−6.69	0.13	1.77	0.512280	0.000008	−6.98	0.15	2.3	0.512296	0.000011	−6.68	0.21	2.05	0.512210	0.000007	−8.34	0.13
701	23,444	0.512319	0.000007	−6.22	0.13	2.07	0.512295	0.000007	−6.68	0.13	2.45	0.512303	0.000007	−6.53	0.13	2.4	0.512146	0.000007	−9.61	0.14

Note. The Nd isotope compositions of the carbonate-free fraction have been also reported. The sediment ages reported in the table are revised using the calibration based on *IntCal20* (Reimer et al., 2020).

Table 3
Nd Isotope Compositions Obtained on Mixed Planktonic Foraminifera in Core MD90-917 (Colin et al., 2021 and This Study)

		Mixed planktonic foraminifera				
Depth (cm)	Age (yrs)	$^{143}Nd/^{144}Nd$	±2sigma	εNd	±2sigma	
18	960	0.512325	0.000018	−6.10	0.35	Colin et al., 2021
61	1,997	0.512333	0.000016	−5.96	0.32	Colin et al., 2021
100	3,094	0.512329	0.000011	−6.02	0.21	Colin et al., 2021
130	3,934	0.512328	0.000009	−6.05	0.18	Colin et al., 2021
179	5,630	0.512326	0.000012	−6.09	0.22	Colin et al., 2021
205	6,525	0.512314	0.000017	−6.33	0.34	Colin et al., 2021
235	7,899	0.512315	0.000019	−6.29	0.37	Colin et al., 2021
249	8,548	0.512331	0.000013	−6.00	0.26	Colin et al., 2021
260	9,708	0.512338	0.000019	−5.85	0.36	Colin et al., 2021
285	11,861	0.512325	0.000013	−6.11	0.25	Colin et al., 2021
310	12,575	0.512349	0.000022	−5.65	0.43	Colin et al., 2021
365	13,486	0.512317	0.000012	−6.26	0.23	Colin et al., 2021
430	15,326	0.512315	0.000014	−6.30	0.28	Colin et al., 2021
460	16,086	0.512311	0.000012	−6.38	0.24	Colin et al., 2021
510	17,831	0.512316	0.000013	−6.29	0.25	Colin et al., 2021
530	18,969	0.512317	0.000013	−6.27	0.25	This study
550	19,823	0.512313	0.000011	−6.35	0.21	Colin et al., 2021
575	20,468	0.512310	0.000013	−6.40	0.25	This study
595	20,768	0.512324	0.000013	−6.12	0.25	This study
635	21,415	0.512307	0.000014	−6.46	0.27	This study
665	22,350	0.512323	0.000013	−6.14	0.25	This study
701	23,444	0.512330	0.000015	−6.01	0.28	This study

The distribution of εNd values of leachate obtained on tephra layers and non-tephra layers with the three leaching procedures used in this study can probably be interpreted as: (a) changes in the Nd isotope compositions of pore water and subsequently authigenic fractions during early diagenesis processes; and (b) extraction of lithogenic Nd from the detrital fraction during the sequential leaching procedure.

Recent studies have demonstrated that diagenesis of sediment can induce benthic flux and even modify the concentrations and isotope compositions of dissolved Nd in bottom water in certain oceanic regions (Abbott, Haley, & McManus, 2015, Abbott et al., 2019; Arsouze et al., 2009; Bayon et al., 2011; Haley et al., 2004). The εNd values of pore waters may differ from those of the bottom waters due to the release of Nd through desorption from particles, reduction of authigenic phases, or dissolution of detrital particles (Abbott, Haley, McManus, et al., 2015, 2019; Haley & Klinkhammer, 2003; Sholkovitz, 1989). Given that volcanic glass shards can be easily dissolved in marine sediments (Schacht et al., 2008), tephra can release lithogenic radiogenic Nd into pore water, which can then diffuse into the sediment and reach the water-sediment interface (Randazzo et al., 2012). Through changes in the oxydo-reduction conditions in the sediment, the radiogenic Nd can be trapped in the Fe-Mn coating, as evidenced by the leaching results.

However, the εNd values of the Fe-Mn coating adhered to planktonic foraminifera showed no variations in relation to the detrital εNd values (Figure 3a). Unfortunately, most of the ash layers, which have a low carbonate content (from 10% to 30%), do not contain enough foraminifera to allow for a systematic analysis of the Nd isotope composition of planktonic foraminifera at the same level as samples that have been leached. Nevertheless, a few foraminiferal εNd values of core MD90-917, obtained in tephra layers at 170, 250, 310 and 595 cm, indicate similar values (within the 2σ error bars) to those of foraminifera samples located in non-tephra layers (Figure 3). The narrow range of authigenic εNd values suggests that the glass-shards in the tephra are not significantly

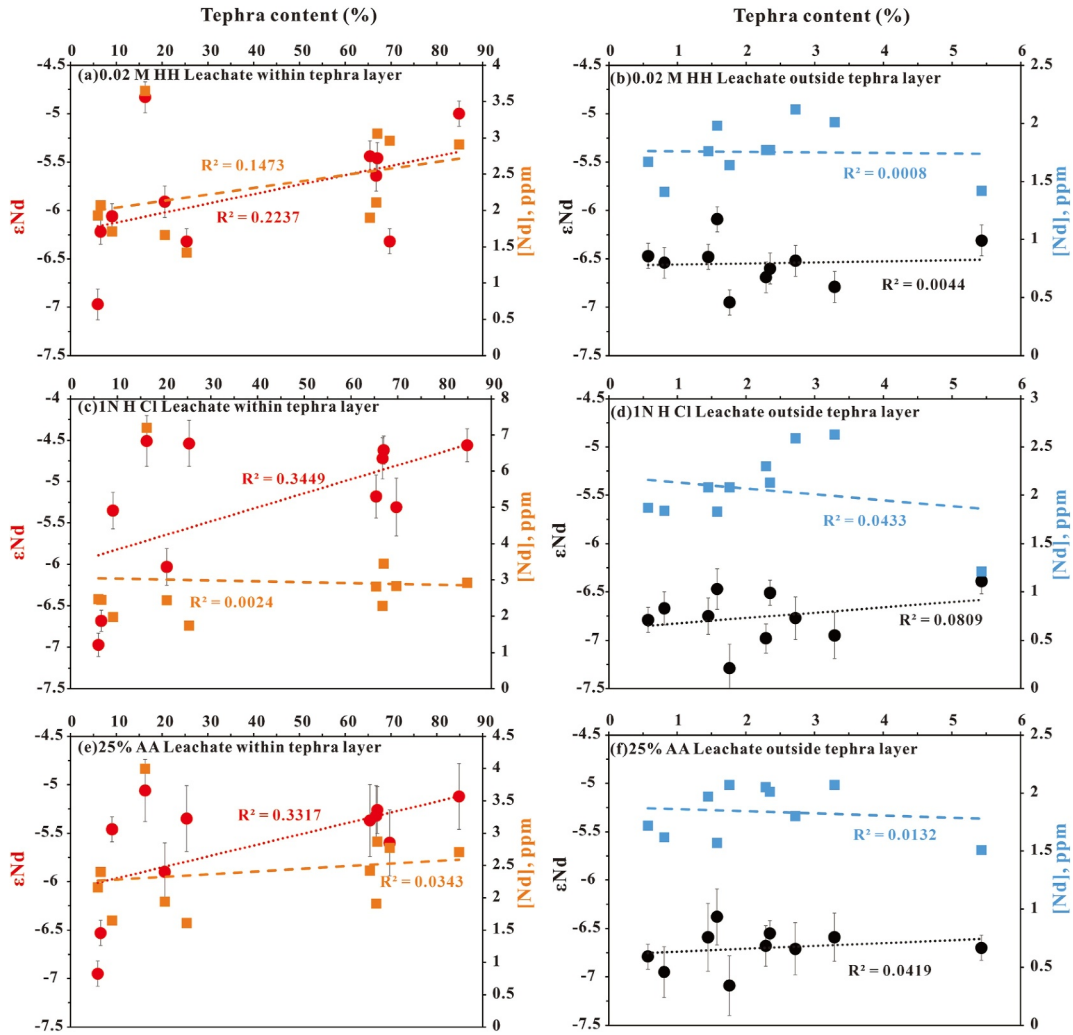

Figure 4. Relationship between tephra content with εNd and [Nd] Nd concentration. (a, c, and e): tephra content vs. [Nd] and εNd for samples within the tephra layers; (b, d, and f): tephra content vs. [Nd] and εNd for samples outside the tephra layers. HH: hydroxylamine hydrochloride; AA: Acetic Acid.

affected by the diagenesis process or dissolution of the tephra. This is consistent with the morphoscopic observations and geochemical analyses of tephra, which indicate that the tephra is unaltered and has not undergone dissolution (Siani et al., 2004).

The other mechanism involves leaching conditions that extract a minor portion of detrital material by dissolution. The extraction of ferromanganese oxyhydroxides from bulk sediments can induce artifacts due to the potential release of non-seawater-derived Nd during the experimental procedure (Bayon et al., 2004; Blaser et al., 2016; Elmore et al., 2011; Molina-Kescher et al., 2014; Roberts et al., 2010; Wilson et al., 2013). During conventional leaching, the volcanogenic fraction of sediments is known to behave as a source of contaminants that has never been quantitatively estimated beforehand (Elmore et al., 2011).

In our study, we used a simple model to quantitatively estimate the contribution of the dissolution of volcanic and non-volcanic detrital materials to the leachate (See Supporting Information S1 for more detail). This contribution is quite low for the tephra layers with an average of 1.4%, 2.0% and 3.8% for the HH, AA and HCl leaching methods, respectively. Moreover, the slightly negative εNd values of leachates for the samples collected on non-tephra layers suggest that the unradiogenic detrital mineral also dissolves during the leaching process (Figure 3b). The average dissolution percentage of unradiogenic detrital minerals is less than 0.2%. By counting the

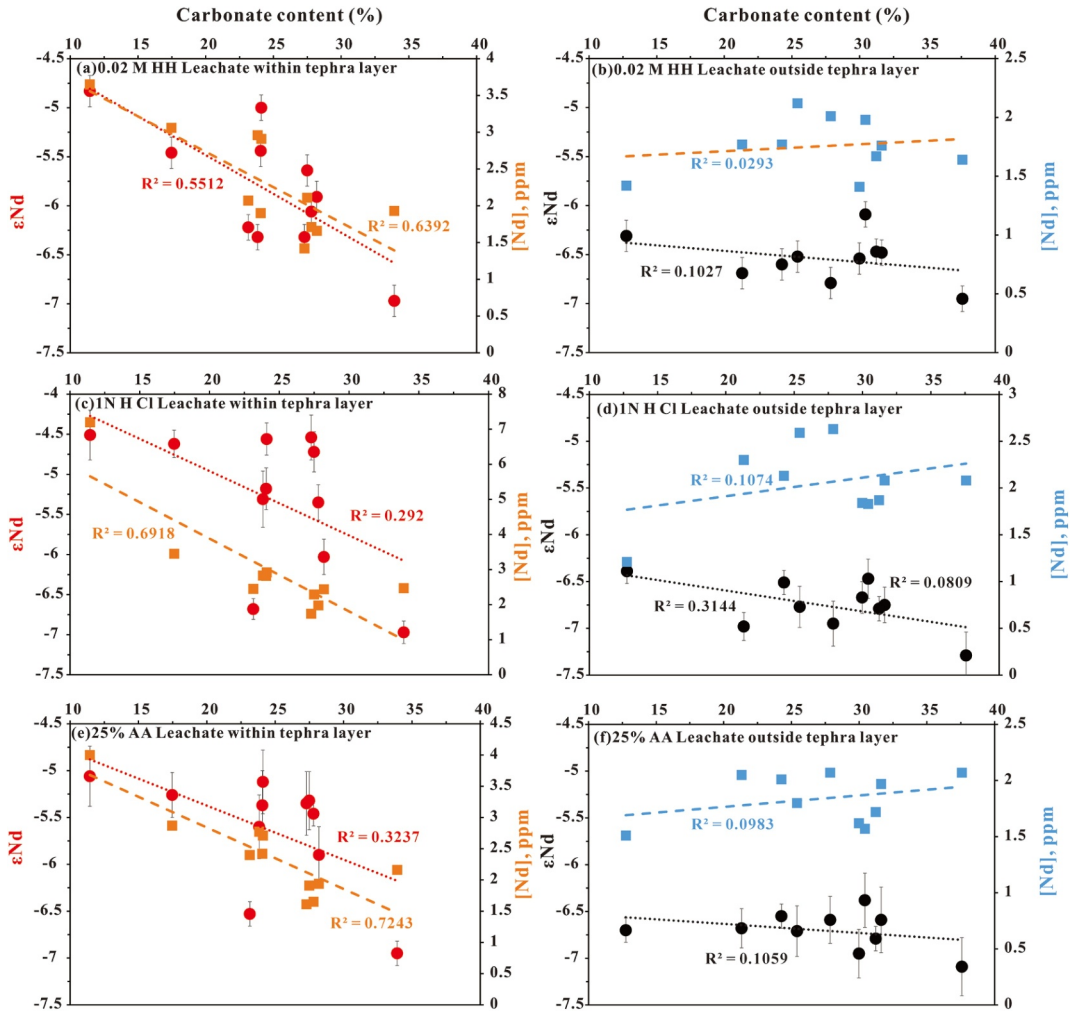

Figure 5. The relationship between carbonate content with εNd and [Nd] concentration. (a, c, and e): carbonate content vs. [Nd] and εNd for samples within the tephra layer; (b, d, and f): carbonate content versus [Nd] and εNd for samples outside the tephra layer. HH: hydroxylamine hydrochloride; AA: Acetic Acid.

dissolution of unradiogenic detrital material, the previous contribution of the dissolution of tephra slightly rises to an average of 2.1%, 2.5% and 4.4% for the HH, AA and HCl, respectively.

Interestingly, evidence of an inverse correlation between the extracted Nd concentration and both carbonate content and εNd is observed for samples taken from tephra layers (Figures 5a, 5c, and 5e). This can be attributed to the preferential dissolution of carbonates in the sediment, which impedes the effective reaction between the leaching solution and volcanogenic components. These findings are corroborated by previous studies indicating that the dissolution rate of basaltic glass can vary by a factor of more than one order of magnitude between pH 4 and pH 7, with the extent of this variation being dependent on the $CaCO_3$ content of the sample (e.g., Gislason & Oelkers, 2003). Our newly acquired results indicate an inverse correlation between the carbonate content versus the percentage contribution of tephra dissolution in the leachate (with a lower contribution when the carbonate contents are higher) (Figures 5a, 5c, and 5e, and 6). This demonstrates that the presence of carbonate helps to prevent volcanic glass dissolution. This finding is consistent with the previous study by Wilson et al. (2013), arguing that the volcanogenic material is a minor reactive component. Regarding changes in εNd values, even slight dissolution of volcanogenic material (average 2.7%) can result in a noticeable modification of εNd values of the leachate since there is a significant disparity between the volcanogenic material and the bottom water signal ($\Delta\varepsilon Nd_{\text{volanic-MD90-917 core top foraminiferal}}$ reaching to 7 unit). In conclusion, the slight dissolution of highly

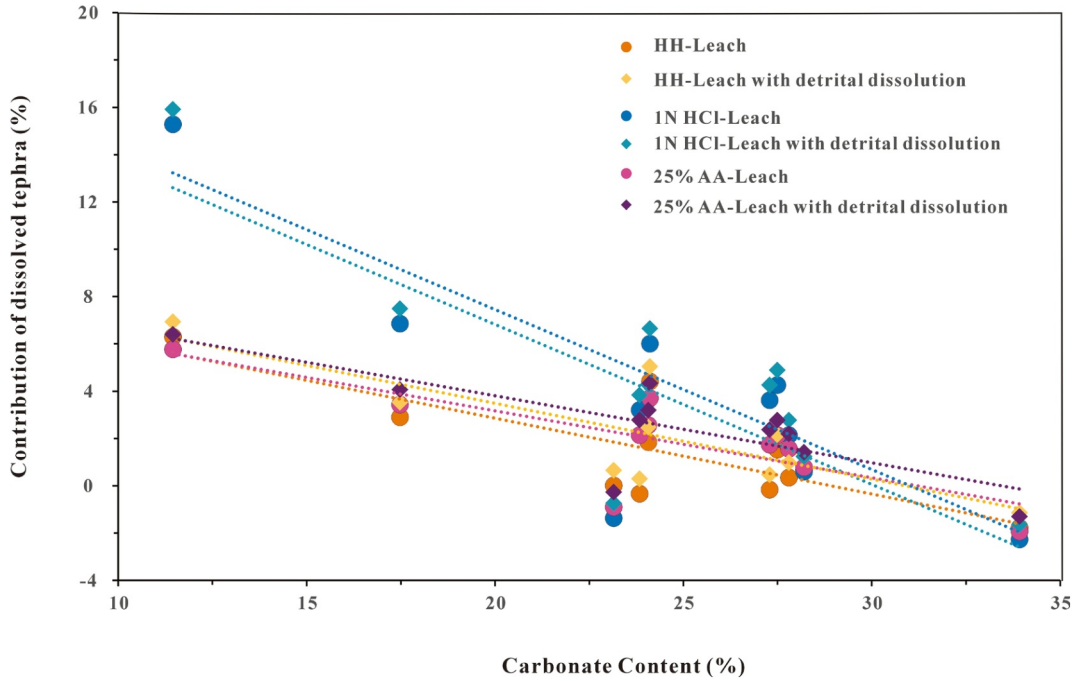

Figure 6. Carbonate content versus the contribution of dissolved tephra (%) on the 1 N HCl leachate (light and dark blue symbols and dashed lines), 25% Acetic Acid leachate (pink and purple symbols and dashed lines) and 0.02 M hydroxylamine hydrochloride (HH) leachate (orange and yellow symbols and dashed lines) from samples collected in tephra layers.

radiogenic tephra under the leaching conditions can modify the εNd values of acid leaches. The process becomes far more pronounced as the carbonate content decreases.

4.2. Evaluation of the Leaching Procedure in Non-Tephra Layers

In the absence of tephra layers, the diagenesis of unradiogenic detrital minerals, such as feldspar dissolution and authigenic clay formation, can result in the enrichment of Nd in pore water. This is followed by the exchange of Nd with authigenic Fe-Mn and phosphate phases (Abbott et al., 2019; Bayon et al., 2015; Caetano et al., 2009; Freydier et al., 2001; Ohr et al., 1994; Schacht et al., 2010; Uysal & Golding, 2003; Wu et al., 2019; Zhong & Mucci, 1995). An offset of −2 epsilon Nd units is observed between the εNd values of the leachate and detrital components, with no change in leachate εNd observed with changes in detrital εNd (Figure 3b). This indicates that the detrital components are not the main phase extracted. Notably, a slight discrepancy exists between the εNd values of planktonic foraminifera and sediment leachates, with the latter exhibiting more unradiogenic values. This suggests that the leachate εNd is influenced by partial extraction of unradiogenic detrital components (average 0.2%). Moreover, there was a slight difference in the dissolution proportion of the three leachates. The average dissolved proportion is 0.18%, 0.31% and 0.4% for the HH, AA and HCl leaching procedures, respectively. The comparison of foraminiferal εNd with those obtained from the three leaching methods reveals that the discrepancy between HCl-leaches εNd and those of the foraminifera is the most pronounced with −0.52, followed by −0.46 for AA-leaches, and a minor value of −0.30 for HH-leaches (Figure 3). In addition, taking experimental error into account, HH-leaches align closely with the values of the foraminifera, while HCl HCl-leaches deviate further away. This suggests that the chemical conditions employed in this study (non-decarbonated samples, weak acid treatment, short leaching time; Blaser et al., 2016; Wilson et al., 2013) are effective in extracting signatures of authigenic Fe-Mn coatings. We can therefore conclude that the HH leaching method applied to bulk sediment from samples taken outside the tephra layers can be successfully used to reconstruct past seawater εNd.

4.3. Seawater εNd Record of the Deep-Water of the Adriatic Sea

The occurrence of sapropel deposition between 6.1 and 10.2 cal kyr BP in the eastern Mediterranean Sea (De Lange et al., 2008) indicates a significant shift in hydrological circulation patterns over this period (Cramp &

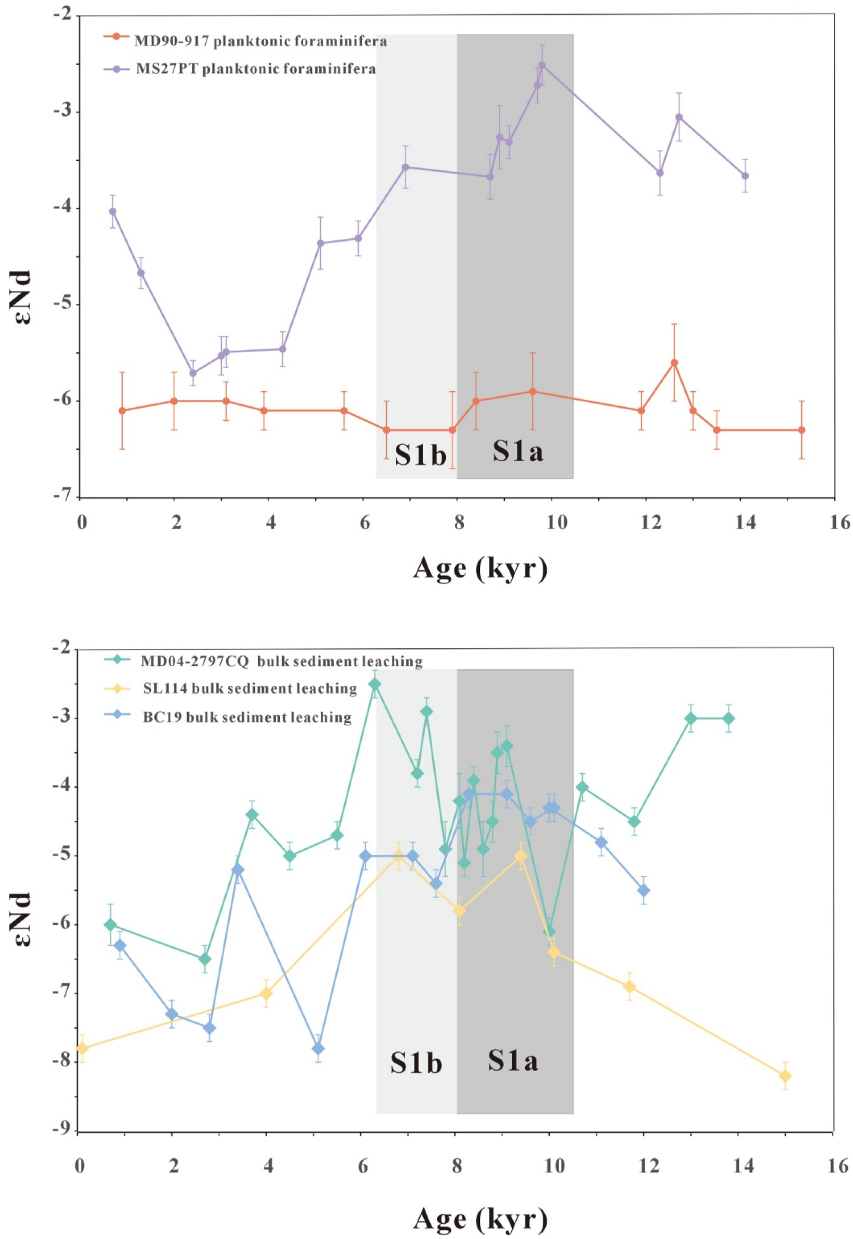

Figure 7. Comparison of εNd records obtained in this study (core MD90-917, purple circles and line, Colin et al., 2021 and this study) and previous εNd records obtained in the EMS and WMS for the last 16 cal kyr BP: core MS27PT (31°47.90'N, 29°27.700E; water depth 1,389 m, orange circles and line) from Duhamel et al. (2020); core MD04-2797CQ (36°57'N, 11° 40'E; 771 m water depth, green diamonds and line) from Cornuault et al. (2018); cores BC19 (33°47.9′ N, 28°36.5′ E; water depth 2,750 m, blue diamonds and line) from Tachikawa et al. (2004) and SL114 (35°17.2′ N, 21°24.5′ E; water depth 3,390 m, yellow diamonds and line) from Wu et al. (2019).

O'Sullivan, 1999; Emeis et al., 1991, 2000; Rossignol-Strick, 1983; Rohling, 1994; Rohling et al., 2015; Schmiedl et al., 2010; Siani et al., 2013; Ziegler et al., 2010) found sapropel S1 deposition in core MD90-917, suggesting similar oxygen-depleted conditions across the Eastern Mediterranean Sea, including the Adriatic Sea. For the core MP27PT (N31°47′90; E29°27′70; water depth 1,389 m, Figure 1), located off the Nile River mouth, the planktonic foraminiferal εNd became more radiogenic during the deposition of S1 as a result of the input of the Nile River and/or the boundary exchange with radiogenic sediments of the eastern Levantine margin (Figure 7; Duhamel et al., 2020). Core BC19 (N33°47.9′; E28°36.5′; water depth 2,750 m, Figure 1; Tachikawa et al., 2004), located in the western Levantine Basin, core SL114 (N35°17.2′; E21°24.5′; water depth 3,390 m, Figure 1; Wu

et al., 2019) located in the Ionian Sea, and core MD04-2797CQ (N36°57′; E11°40′; water depth 771 m, Figure 1; Cornuault et al., 2018) located in the central Mediterranean Sea, exhibited a similar trend with the bulk sediment leachate εNd becoming more radiogenic during the sapropel S1 deposition (Figure 7).

Previous studies in the EMS have shown that the radiogenic volcanic Nile River sediments decrease sharply westward from the river's mouth toward the Mediterranean Ridge situated near Crete (Blanchet, 2019; Krom et al., 1999; Weldeab et al., 2002). The radiogenic εNd value observed in all the records of the EMS and Tyrrhenian Sea between 600 and 2,500 m water depth is the result of the circulation of the radiogenic εNd of the LIW to both basins of the Mediterranean Sea coupled with a decrease of the deep-water ventilation in the EMS inducing a longer time of contact between seawater and the radiogenic sediments of the eastern and southern margins of the Levantine Basin (Colin et al., 2021; Wu et al., 2018).

However, the planktonic foraminiferal εNd of core MD90-917 remains almost constant during the last 20 kyr (Figure 7), indicating that it records a local signature. The Adriatic Sea is surrounded by unradiogenic sediment margins (Ayache et al., 2016). This suggests that the radiogenic LIW, which have already been strongly modified by mixing with more unradiogenic water masses above (MAW) and below, cannot impact the deep-water Nd isotope compositions formed in the Adriatic Sea. This is consistent with the modern seawater εNd profiles, which do not display any discernible radiogenic εNd LIW in the southern Adriatic Sea (Montagna et al., 2022). Consequently, the low deep-water ventilation state during the sapropel S1 could be also favorable for greater exchanges between seawater and sediment and induced a local seawater Nd isotope composition with stable unradiogenic Nd isotope composition in the Adriatic Sea and more radiogenic one for the Southeastern Levantine Basin where the main detrital source near the Nile deep-sea fan derive mainly from the radiogenic volcanic material from the Blue Nile River (from 0 to +7, Garzanti et al., 2015). The contribution of the latter increases at 15 cal ka BP with the onset of the african humid period and peaks during the sapropel S1 deposition (Revel et al., 2010, 2014) which also particiape to increased the εNd gradient of deep-water masses between the Southeastern Levantine Basin and the western Mediterranean Sea (Figure 7).

After the sapropel S1 deposition, the planktonic foraminiferal εNd of core MP27PT was similar to that of core MD90-917. This finding suggests the presence of active ventilation in the EMS and deep-water masses, which are primarily sourced from the Adriatic Sea (Filippidi et al., 2016; Schmiedl et al., 2010; Siani et al., 2013) (Figure 7). In general, the bulk sediment leachate εNd records obtained in the EMS display a similar tendency despite a higher degree of variability and absolute εNd values that may be attributed to the potential contribution of detrital sediments during leaching processes.

5. Conclusion

We investigated the impact of volcanic tephra layers on authigenic neodymium isotope composition (εNd) extracted by different analytical procedures of a sedimentary sequence of the South Adriatic deep basin with well-identified tephra layers to evaluate the different analytical procedures. Authigenic εNd have been extracted from mix planktonic foraminifera samples and non-decarbonated sediment leachates obtained with three solutions commonly used in the context of the Mediterranean Sea: (a) 0.02 M hydroxylamine hydrochloride (HH) solution, (b) 1N HCl, and (c) a 25% (v/v) acetic acid (AA).

The normalized-REE patterns exhibit a MREE enrichment pattern, suggesting that Fe-Mn coatings are the primary phase present in the extracted leachate. However, the leachates' εNd and high HREE/LREE ratio indicate the dissolution of the tephra layers in the extracted phase. These findings indicate that sediments with higher tephra contents result in more radiogenic Nd signatures of the authigenic fraction extracted from acid-leachates. Interestingly, despite the extensive accumulation of ash layers in the Adriatic Sea sediments, the εNd values of foraminifera exhibit no discernible variations over the past 20 kyr BP. This suggests that diagenesis of volcanic ash deposits is unlikely to be the main process responsible for the more radiogenic εNd values observed in the acid-leachates. Instead, it appears that sequential extraction may be capable of dissolving a minor amount of tephra during weak acid attacks, resulting in slightly more radiogenic leachate values.

We emphasized the importance of considering the different leaching methods and their associated biases when extracting seawater εNd from sediments. A comparison of the leaching results with the foraminiferal εNd values revealed that the hydroxylamine hydrochloride (HH) leaching method was particularly effective, closely matching the foraminiferal εNd. In contrast, leaching with HCl displayed a greater deviation, indicating the need

for careful evaluation of leaching procedures on a site-specific basis. In summary, our results confirm that the most reliable analytical leaching method involves non-decarbonated samples, weak acid treatment, and a short leaching time in sediment sequences characterized by abundant deposits of tephra layers.

The foraminiferal εNd values of core MD90-917 remain constant over the last 20 cal kyr BP, suggesting that the Adriatic deep-water predominantly reflects local characteristics since the last glacial period. A comparison of foraminiferal εNd records of the southeastern Levantine Basin and the Adriatic Sea reveals a large gradient, which is consistent with the hypothesis of low ventilation and local Nd isotope signature resulting from the dissolution of radiogenic volcanic material in the southeastern Levantine Basin and unradiogenic sediments along the Adriatic Sea margin. The time interval following the deposition of sapropel S1 is characterized by a homogeneous unradiogenic εNd value for deep-water across the Eastern Mediterranean Sea, indicating active ventilation and deep-water masses originating mainly from the Adriatic Sea.

Data Availability Statement

Data supporting this paper are available in the following Data Repository: Gao et al. (2024), https://doi.org/10.17632/c7xbkzvs9y.1.

Acknowledgments
The research leading to this paper was funded by the French National Research Agency under the "Investissements d'avenir" programme (Grant ANR-11-IDEX-0004-17-EURE-0006), the MEDSENS Project (Grant ANR-19-CE01-0019) and the INSU LEFE-IMAGO PALMEDS Project. We gratefully acknowledge the support provided by Louise Bordier during the Nd isotope composition analyses. We especially thank two anonymous reviewers for their constructive reviews, which significantly helped to improve this manuscript.

References

Abbott, A. N., Haley, B. A., & McManus, J. (2015). Bottoms up: Sedimentary control of the deep north Pacific Ocean's εNd signature. *Geology*, *43*(11), 1035. https://doi.org/10.1130/G37114.1

Abbott, A. N., Haley, B. A., McManus, J., & Reimers, C. E. (2015). The sedimentary flux of dissolved rare earth elements to the ocean. *Geochimica et Cosmochimica Acta*, *154*, 186–200. https://doi.org/10.1016/j.gca.2015.01.010

Abbott, A. N., Löhr, S., & Trethewy, M. (2019). Are clay minerals the primary control on the oceanic rare earth element budget? *Frontiers in Marine Science*, *6*, 504. https://doi.org/10.3389/fmars.2019.00504

Arsouze, T., Dutay, J. C., Lacan, F., & Jeandel, C. (2009). Reconstructing the Nd oceanic cycle using a coupled dynamical–biogeochemical model. *Biogeosciences*, *6*(12), 2829–2846. https://doi.org/10.5194/bg-6-2829-2009

Ayache, M., Dutay, J. C., Arsouze, T., Révillon, S., Beuvier, J., & Jeandel, C. (2016). High-resolution neodymium characterization along the Mediterranean margins and modelling of ε Nd distribution in the Mediterranean basins. *Biogeosciences*, *13*(18), 5259–5276. https://doi.org/10.5194/bg-13-5259-2016

Ayuso, R. A., De Vivo, B., Rolandi, G., Seal II, R. R., & Paone, A. (1998). Geochemical and isotopic (Nd–Pb–Sr–O) variations bearing on the genesis of volcanic rocks from Vesuvius, Italy. *Journal of Volcanology and Geothermal Research*, *82*(1–4), 53–78. https://doi.org/10.1016/S0377-0273(97)00057-7

Bau, M., Möller, P., & Dulski, P. (1997). Yttrium and lanthanides in eastern Mediterranean seawater and their fractionation during redox-cycling. *Marine Chemistry*, *56*(1–2), 123–131. https://doi.org/10.1016/S0304-4203(96)00091-6

Bayon, G., Birot, D., Ruffine, L., Caprais, J. C., Ponzevera, E., Bollinger, C., et al. (2011). Evidence for intense REE scavenging at cold seeps from the Niger Delta margin. *Earth and Planetary Science Letters*, *312*(3–4), 443–452. https://doi.org/10.1016/j.epsl.2011.10.008

Bayon, G., German, C. R., Boella, R. M., Milton, J. A., Taylor, R. N., & Nesbitt, R. W. (2002). An improved method for extracting marine sediment fractions and its application to Sr and Nd isotopic analysis. *Chemical Geology*, *187*(3–4), 179–199. https://doi.org/10.1016/S0009-2541(01)00416-8

Bayon, G., German, C. R., Burton, K. W., Nesbitt, R. W., & Rogers, N. (2004). Sedimentary Fe–Mn oxyhydroxides as paleoceanographic archives and the role of aeolian flux in regulating oceanic dissolved REE. *Earth and Planetary Science Letters*, *224*(3–4), 477–492. https://doi.org/10.1016/j.epsl.2004.05.033

Bayon, G., Toucanne, S., Skonieczny, C., André, L., Bermell, S., Cheron, S., et al. (2015). Rare earth elements and neodymium isotopes in world river sediments revisited. *Geochimica et Cosmochimica Acta*, *170*, 17–38. https://doi.org/10.1016/j.gca.2015.08.001

Blanchet, C. L. (2019). A database of marine and terrestrial radiogenic Nd and Sr isotopes for tracing earth-surface processes. *Earth System Science Data*, *11*(2), 741–759. https://doi.org/10.5194/essd-11-741-2019

Blaser, P., Lippold, J., Gutjahr, M., Frank, N., Link, J. M., & Frank, M. (2016). Extracting foraminiferal seawater Nd isotope signatures from bulk deep sea sediment by chemical leaching. *Chemical Geology*, *439*, 189–204. https://doi.org/10.1016/j.chemgeo.2016.06.024

Bourne, A. J., Lowe, J. J., Trincardi, F., Asioli, A., Blockley, S. P. E., Wulf, S., et al. (2010). Distal tephra record for the last ca 105,000 years from core PRAD 1-2 in the central Adriatic Sea: Implications for marine tephrostratigraphy. *Quaternary Science Reviews*, *29*(23–24), 3079–3094. https://doi.org/10.1016/j.quascirev.2010.07.021

Broecker, W. S., & Peng, T. H. (1982). *Tracers in the sea* (Vol. 690). Lamont-Doherty Geological Observatory, Columbia University.

Caetano, M., Prego, R., Vale, C., de Pablo, H., & Marmolejo-Rodríguez, J. (2009). Record of diagenesis of rare earth elements and other metals in a transitional sedimentary environment. *Marine Chemistry*, *116*(1–4), 36–46. https://doi.org/10.1016/j.marchem.2009.09.003

Calanchi, N., & Dinelli, E. (2008). Tephrostratigraphy of the last 170 ka in sedimentary successions from the Adriatic Sea. *Journal of Volcanology and Geothermal Research*, *177*(1), 81–95. https://doi.org/10.1016/j.jvolgeores.2008.06.008

Censi, P., Zuddas, P., Larocca, D., Saiano, F., Placenti, F., & Bonanno, A. (2007). Recognition of water masses according to geochemical signatures in the central Mediterranean Sea: Y/Ho ratio and rare earth element behaviour. *Chemistry and Ecology*, *23*(2), 139–153. https://doi.org/10.1080/02757540701197879

Colin, C., Duhamel, M., Siani, G., Dubois-Dauphin, Q., Ducassou, E., Liu, Z., et al. (2021). Changes in the intermediate water masses of the Mediterranean Sea during the last climatic cycle—New constraints from neodymium isotopes in foraminifera. *Paleoceanography and Paleoclimatology*, *36*(4), e2020PA004153. https://doi.org/10.1029/2020PA004153

Copard, K., Colin, C., Douville, E., Freiwald, A., Gudmundsson, G., De Mol, B., & Frank, N. (2010). Nd isotopes in deep-sea corals in the North-eastern Atlantic. *Quaternary Science Reviews*, *29*(19–20), 2499–2508. https://doi.org/10.1016/j.quascirev.2010.05.025

Cornuault, M., Tachikawa, K., Vidal, L., Guihou, A., Siani, G., Deschamps, P., et al. (2018). Circulation changes in the eastern Mediterranean Sea over the past 23,000 years inferred from authigenic Nd isotopic ratios. *Paleoceanography and Paleoclimatology*, *33*(3), 264–280. https://doi.org/10.1002/2017pa003227

Cramp, A., & O'Sullivan, G. (1999). Neogene sapropels in the mediterranean: A review. *Marine Geology*, *153*(1–4), 11–28. https://doi.org/10.1016/S0025-3227(98)00092-9

Crocket, K. C., Vance, D., Gutjahr, M., Foster, G. L., & Richards, D. A. (2011). Persistent nordic deep-water overflow to the glacial north Atlantic. *Geology*, *39*(6), 515–518. https://doi.org/10.1130/G31677.1

Crovisier, J. L., Honnorez, J., & Eberhart, J. P. (1987). Dissolution of basaltic glass in seawater: Mechanism and rate. *Geochimica et Cosmochimica Acta*, *51*(11), 2977–2990. https://doi.org/10.1016/0016-7037(87)90371-1

D'Antonio, M., Mariconte, R., Arienzo, I., Mazzeo, F. C., Carandente, A., Perugini, D., et al. (2016). Combined Sr-Nd isotopic and geochemical fingerprinting as a tool for identifying tephra layers: Application to deep-sea cores from Eastern Mediterranean Sea. *Chemical Geology*, *443*, 121–136. https://doi.org/10.1016/j.chemgeo.2016.09.022

D'Antonio, M., Tonarini, S., Arienzo, I., Civetta, L., & Di Renzo, V. (2007). Components and processes in the magma genesis of the Phlegrean Volcanic District, southern Italy. https://doi.org/10.1130/2007.2418(10)

De Lange, G. J., Thomson, J., Reitz, A., Slomp, C. P., Speranza Principato, M., Erba, E., & Corselli, C. (2008). Synchronous basin-wide formation and redox-controlled preservation of a Mediterranean sapropel. *Nature Geoscience*, *1*(9), 606–610. https://doi.org/10.1038/ngeo291

Du, J., Haley, B. A., & Mix, A. C. (2016). Neodymium isotopes in authigenic phases, bottom waters and detrital sediments in the Gulf of Alaska and their implications for paleo-circulation reconstruction. *Geochimica et Cosmochimica Acta*, *193*, 14–35. https://doi.org/10.1016/j.gca.2016.08.005

Dubois-Dauphin, Q., Montagna, P., Siani, G., Douville, E., Wienberg, C., Hebbeln, D., et al. (2017). Hydrological variations of the intermediate water masses of the western Mediterranean Sea during the past 20 ka inferred from neodymium isotopic composition in foraminifera and cold-water corals. *Climate of the Past*, *13*(1), 17–37. https://doi.org/10.5194/cp-13-17-2017

Duhamel, M., Colin, C., Revel, M., Siani, G., Dapoigny, A., Douville, É., et al. (2020). Variations in eastern Mediterranean hydrology during the last climatic cycle as inferred from neodymium isotopes in foraminifera. *Quaternary Science Reviews*, *237*, 106306. https://doi.org/10.1016/j.quascirev.2020.106306

Elderfield, H., Hawkesworth, C. J., Greaves, M. J., & Calvert, S. E. (1981). Rare earth element geochemistry of oceanic ferromanganese nodules and associated sediments. *Geochimica et Cosmochimica Acta*, *45*(4), 513–528. https://doi.org/10.1016/0016-7037(81)90184-8

Elderfield, H., & Sholkovitz, E. T. (1987). Rare earth elements in the pore waters of reducing nearshore sediments. *Earth and Planetary Science Letters*, *82*(3–4), 280–288. https://doi.org/10.1016/0012-821X(87)90202-0

Elmore, A. C., Piotrowski, A. M., Wright, J. D., & Scrivner, A. E. (2011). Testing the extraction of past seawater Nd isotopic composition from North Atlantic deep sea sediments and foraminifera. *Geochemistry, Geophysics, Geosystems*, *12*(9). https://doi.org/10.1029/2011GC003741

Emeis, K. C., Camerlenghi, A., McKenzie, J. A., Rio, D., & Sprovieri, R. (1991). The occurrence and significance of pleistocene and upper pliocene sapropels in the Tyrrhenian Sea. *Marine Geology*, *100*(1–4), 155–182. https://doi.org/10.1016/0025-3227(91)90231-R

Emeis, K. C., Struck, U., Schulz, H. M., Rosenberg, R., Bernasconi, S., Erlenkeuser, H., et al. (2000). Temperature and salinity variations of Mediterranean Sea surface waters over the last 16,000 years from records of planktonic stable oxygen isotopes and alkenone unsaturation ratios. *Palaeogeography, Palaeoclimatology, Palaeoecology*, *158*(3–4), 259–280. https://doi.org/10.1016/S0031-0182(00)00053-5

Filippidi, A., Triantaphyllou, M. V., & De Lange, G. J. (2016). Eastern-Mediterranean ventilation variability during sapropel S1 formation, evaluated at two sites influenced by deep-water formation from Adriatic and Aegean Seas. *Quaternary Science Reviews*, *144*, 95–106. https://doi.org/10.1016/j.quascirev.2016.05.024

Frank, M. (2002). Radiogenic isotopes: Tracers of past ocean circulation and erosional input. *Reviews of Geophysics*, *40*(1), 1. https://doi.org/10.1029/2000RG000094

Freydier, R., Michard, A., De Lange, G., & Thomson, J. (2001). Nd isotopic compositions of eastern mediterranean sediments: Tracers of the nile influence during sapropel S1 formation? *Marine Geology*, *177*(1–2), 45–62. https://doi.org/10.1016/S0025-3227(01)00123-2

Gao, G., Colin, C., Siani, G., Sepulcre, S., Pinna, R., Haurine, F., & Dapoigny, A. (2024). Extracting Nd isotope signatures from bulk deep-sea sediment with ash-layers by chemical leaching: A case study in the Adriatic Se. *Mendeley Data*. https://doi.org/10.17632/c7xbkzvs9y.1

Garcia-Solsona, E., Pena, L. D., Paredes, E., Pérez-Asensio, J. N., Quirós-Collazos, L., Lirer, F., & Cacho, I. (2020). Rare earth elements and Nd isotopes as tracers of modern ocean circulation in the central Mediterranean Sea. *Progress in Oceanography*, *185*, 102340. https://doi.org/10.1016/j.pocean.2020.102340

Garzanti, E., Andò, S., Padoan, M., Vezzoli, G., & El Kammar, A. (2015). The modern Nile sediment system: Processes and products. *Quaternary Science Reviews*, *130*, 9–56. https://doi.org/10.1016/j.quascirev.2015.07.011

Gieskes, J. M., Vrolijk, P., & Blanc, G. (1990). Hydrogeochemistry of the northern Barbados accretionary complex transect: Ocean Drilling Project Leg 110. *Journal of Geophysical Research*, *95*(B6), 8809–8818. https://doi.org/10.1029/JB095iB06p08809

Gislason, S. R., & Oelkers, E. H. (2003). Mechanism, rates, and consequences of basaltic glass dissolution: II. An experimental study of the dissolution rates of basaltic glass as a function of pH and temperature. *Geochimica et Cosmochimica Acta*, *67*(20), 3817–3832. https://doi.org/10.1016/S0016-7037(03)00176-5

Goldstein, S. J., & Jacobsen, S. B. (1987). The Nd and Sr isotopic systematics of river-water dissolved material: Implications for the sources of Nd and Sr in seawater. *Chemical Geology: Isotope Geoscience section*, *66*(3–4), 245–272. https://doi.org/10.1016/0168-9622(87)90045-5

Goldstein, S. L., & Hemming, S. R. (2003). Long-lived isotopic tracers in oceanography, paleoceanography, and ice-sheet dynamics. *Treatise on geochemistry*, *6*, 625. https://doi.org/10.1016/B0-08-043751-6/06179-X

Grenier, M., Brown, K. A., Colombo, M., Belhadj, M., Baconnais, I., Pham, V., et al. (2022). Controlling factors and impacts of river-borne neodymium isotope signatures and rare earth element concentrations supplied to the Canadian Arctic Archipelago. *Earth and Planetary Science Letters*, *578*, 117341. https://doi.org/10.1016/j.epsl.2021.117341

Grousset, F. E., Biscaye, P. E., Zindler, A., Prospero, J., & Chester, R. (1988). Neodymium isotopes as tracers in marine sediments and aerosols: North Atlantic. *Earth and Planetary Science Letters*, *87*(4), 367–378. https://doi.org/10.1016/0012-821X(88)90001-5

Gutjahr, M., Frank, M., Stirling, C. H., Klemm, V., Van de Flierdt, T., & Halliday, A. N. (2007). Reliable extraction of a deepwater trace metal isotope signal from Fe–Mn oxyhydroxide coatings of marine sediments. *Chemical Geology*, *242*(3–4), 351–370. https://doi.org/10.1016/j.chemgeo.2007.03.021

Haley, B. A., & Klinkhammer, G. P. (2003). Complete separation of rare earth elements from small volume seawater samples by automated ion chromatography: Method development and application to benthic flux. *Marine Chemistry*, *82*(3–4), 197–220. https://doi.org/10.1016/S0304-4203(03)00070-7

Haley, B. A., Klinkhammer, G. P., & McManus, J. (2004). Rare earth elements in pore waters of marine sediments. *Geochimica et Cosmochimica Acta*, *68*(6), 1265–1279. https://doi.org/10.1016/j.gca.2003.09.012

Henry, F., Jeandel, C., Dupré, B., & Minster, J. F. (1994). Particulate and dissolved Nd in the western Mediterranean Sea: Sources, fate and budget. *Marine Chemistry*, *45*(4), 283–305. https://doi.org/10.1016/0304-4203(94)90075-2

Jacobsen, S. B., & Wasserburg, G. J. (1980). Sm-Nd isotopic evolution of chondrites. *Earth and Planetary Science Letters*, *50*(1), 139–155. https://doi.org/10.1016/0012-821X(80)90125-9

Jeandel, C., Peucker-Ehrenbrink, B., Jones, M. T., Pearce, C. R., Oelkers, E. H., Godderis, Y., et al. (2011). Ocean margins: The missing term in oceanic element budgets? *Eos, Transactions American Geophysical Union*, *92*(26), 217–218. https://doi.org/10.1029/2011EO260001

Jiménez-Espejo, F. J., Pardos-Gené, M., Martínez-Ruiz, F., García-Alix, A., Van de Flierdt, T., Toyofuku, T., et al. (2015). Geochemical evidence for intermediate water circulation in the westernmost Mediterranean over the last 20 kyr BP and its impact on the Mediterranean Outflow. *Global and Planetary Change*, *135*, 38–46. https://doi.org/10.1016/j.gloplacha.2015.10.001

Kent, A. J., Norman, M. D., Hutcheon, I. D., & Stolper, E. M. (1999). Assimilation of seawater-derived components in an oceanic volcano: Evidence from matrix glasses and glass inclusions from Loihi seamount, Hawaii. *Chemical Geology*, *156*(1–4), 299–319. https://doi.org/10.1016/S0009-2541(98)00188-0

Krom, M. D., Cliff, R. A., Eijsink, L. M., Herut, B., & Chester, R. (1999). The characterisation of Saharan dusts and Nile particulate matter in surface sediments from the Levantine basin using Sr isotopes. *Marine Geology*, *155*(3–4), 319–330. https://doi.org/10.1016/S0025-3227(98)00130-3

Lacan, F., & Jeandel, C. (2005a). Acquisition of the neodymium isotopic composition of the north Atlantic deep water. *Geochemistry, Geophysics, Geosystems*, *6*(12). https://doi.org/10.1029/2005GC000956

Lacan, F., & Jeandel, C. (2005b). Neodymium isotopes as a new tool for quantifying exchange fluxes at the continent–ocean interface. *Earth and Planetary Science Letters*, *232*(3–4), 245–257. https://doi.org/10.1016/j.epsl.2005.01.004

Malusà, M. G., Wang, J., Garzanti, E., Liu, Z. C., Villa, I. M., & Wittmann, H. (2017). Trace-element and Nd-isotope systematics in detrital apatite of the Po river catchment: Implications for provenance discrimination and the lag-time approach to detrital thermochronology. *Lithos*, *290*, 48–59. https://doi.org/10.1016/j.lithos.2017.08.006

Martin, E. E., Blair, S. W., Kamenov, G. D., Scher, H. D., Bourbon, E., Basak, C., & Newkirk, D. N. (2010). Extraction of Nd isotopes from bulk deep sea sediments for paleoceanographic studies on Cenozoic time scales. *Chemical Geology*, *269*(3–4), 414–431. https://doi.org/10.1016/j.chemgeo.2009.10.016

Matthews, I. P., Trincardi, F., Lowe, J. J., Bourne, A. J., MacLeod, A., Abbott, P. M., et al. (2015). Developing a robust tephrochronological framework for late quaternary marine records in the southern Adriatic Sea: New data from core station SA03-11. *Quaternary Science Reviews*, *118*, 84–104. https://doi.org/10.1016/j.quascirev.2014.10.009

Molina-Kescher, M., Frank, M., & Hathorne, E. (2014). South Pacific dissolved Nd isotope compositions and rare earth element distributions: Water mass mixing versus biogeochemical cycling. *Geochimica et Cosmochimica Acta*, *127*, 171–189. https://doi.org/10.1016/j.gca.2013.11.038

Montagna, P., Colin, C., Frank, M., Störling, T., Tanhua, T., Rijkenberg, M. J., et al. (2022). Dissolved neodymium isotopes in the Mediterranean Sea. *Geochimica et Cosmochimica Acta*, *322*, 143–169. https://doi.org/10.1016/j.gca.2022.01.005

Morin, G. P., Vigier, N., & Verney-Carron, A. (2015). Enhanced dissolution of basaltic glass in brackish waters: Impact on biogeochemical cycles. *Earth and Planetary Science Letters*, *417*, 1–8. https://doi.org/10.1016/j.epsl.2015.02.005

Nance, W. B., & Taylor, S. R. (1976). Rare earth element patterns and crustal evolution—I. Australian post-Archean sedimentary rocks. *Geochimica et Cosmochimica Acta*, *40*(12), 1539–1551. https://doi.org/10.1016/0016-7037(76)90093-4

Ohr, M., Halliday, A. N., & Peacor, D. R. (1994). Mobility and fractionation of rare earth elements in argillaceous sediments: Implications for dating diagenesis and low-grade metamorphism. *Geochimica et Cosmochimica Acta*, *58*(1), 289–312. https://doi.org/10.1016/0016-7037(94)90465-0

O'nions, R. K., Hamilton, P. J., & Evensen, N. M. (1977). Variations in $^{143}Nd/^{144}Nd$ and $^{87}Sr/^{86}Sr$ ratios in oceanic basalts. *Earth and Planetary Science Letters*, *34*(1), 13–22. https://doi.org/10.1016/0012-821X(77)90100-5

Osborne, A. H., Marino, G., Vance, D., & Rohling, E. J. (2010). Eastern mediterranean surface water Nd during Eemian sapropel S5: Monitoring northerly (mid-latitude) versus southerly (sub-tropical) freshwater contributions. *Quaternary Science Reviews*, *29*(19–20), 2473–2483. https://doi.org/10.1016/j.quascirev.2010.05.015

Palmer, M. R. (1985). Rare earth elements in foraminifera tests. *Earth and Planetary Science Letters*, *73*(2–4), 285–298. https://doi.org/10.1016/0012-821X(85)90077-9

Palmer, M. R., & Elderfield, H. (1986). Rare earth elements and neodymium isotopes in ferromanganese oxide coatings of Cenozoic foraminifera from the Atlantic Ocean. *Geochimica et Cosmochimica Acta*, *50*(3), 409–417. https://doi.org/10.1016/0016-7037(86)90194-8

Paterne, M., Guichard, F., & Labeyrie, J. (1988). Explosive activity of the South Italian volcanoes during the past 80,000 years as determined by marine tephrochronology. *Journal of Volcanology and Geothermal Research*, *34*(3–4), 153–172. https://doi.org/10.1016/0377-0273(88)90030-3

Pattan, J. N., & Parthiban, G. (2007). Do manganese nodules grow or dissolve after burial? Results from the central Indian ocean basin. *Journal of Asian Earth Sciences*, *30*(5–6), 696–705. https://doi.org/10.1016/j.jseaes.2007.03.003

Pichler, T., Veizer, J., & Hall, G. E. (1999). The chemical composition of shallow-water hydrothermal fluids in Tutum Bay, Ambitle Island, Papua New Guinea and their effect on ambient seawater. *Marine Chemistry*, *64*(3), 229–252. https://doi.org/10.1016/S0304-4203(98)00076-0

Piepgras, D. J., & Wasserburg, G. J. (1987). Rare earth element transport in the western North Atlantic inferred from Nd isotopic observations. *Geochimica et Cosmochimica Acta*, *51*(5), 1257–1271. https://doi.org/10.1016/0016-7037(87)90217-1

Piotrowski, A. M., Galy, A., Nicholl, J. A. L., Roberts, N., Wilson, D. J., Clegg, J. A., & Yu, J. (2012). Reconstructing deglacial North and South Atlantic deep water sourcing using foraminiferal Nd isotopes. *Earth and Planetary Science Letters*, *357*, 289–297. https://doi.org/10.1016/j.epsl.2012.09.036

Piotrowski, A. M., Goldstein, S. L., Hemming, S. R., & Fairbanks, R. G. (2004). Intensification and variability of ocean thermohaline circulation through the last deglaciation. *Earth and Planetary Science Letters*, *225*(1–2), 205–220. https://doi.org/10.1016/j.epsl.2004.06.002

Piotrowski, A. M., Goldstein, S. L., Sidney, R. H., Fairbanks, R. G., & Zylberberg, D. R. (2008). Oscillating glacial northern and southern deep water formation from combined neodymium and carbon isotopes. *Earth and Planetary Science Letters*, *272*(1–2), 394–405. https://doi.org/10.1016/j.epsl.2008.05.011

Randazzo, L. A., Saiano, F., Zuddas, P., & Censi, P. (2012). The behaviour of Rare Earth Elements during the volcanic ash dissolution in seawater solution. *Procedia Earth and Planetary Science*, *7*, 721–724. https://doi.org/10.1016/j.proeps.2013.02.001

Reimer, P. J., Austin, W. E., Bard, E., Bayliss, A., Blackwell, P. G., Ramsey, C. B., et al. (2020). The IntCal20 Northern Hemisphere radiocarbon age calibration curve (0–55 cal kBP). *Radiocarbon*, *62*(4), 725–757. https://doi.org/10.1017/RDC.2020.41

Revel, M., Colin, C., Bernasconi, S., Combourieu-Nebout, N., Ducassou, E., Grousset, F. E., et al. (2014). 21,000 years of Ethiopian African monsoon variability recorded in sediments of the western Nile deep-sea fan. *Regional Environmental Change*, *14*(5), 1685–1696. https://doi.org/10.1007/s10113-014-0588-x

Revel, M., Ducassou, E., Grousset, F. E., Bernasconi, S. M., Migeon, S., Révillon, S., et al. (2010). 100,000 years of African monsoon variability recorded in sediments of the Nile margin. *Quaternary Science Reviews*, *29*(11–12), 1342–1362. https://doi.org/10.1016/j.quascirev.2010.02.006

Roberts, N. L., Piotrowski, A. M., McManus, J. F., & Keigwin, L. D. (2010). Synchronous deglacial overturning and water mass source changes. *Science*, *327*(5961), 75–78. https://doi.org/10.1126/science.117806

Robinson, S., Ivanovic, R., van de Flierdt, T., Blanchet, C. L., Tachikawa, K., Martin, E. E., et al. (2021). Global continental and marine detrital εNd: An updated compilation for use in understanding marine Nd cycling. *Chemical Geology*, *567*, 120119. https://doi.org/10.1016/j.chemgeo.2021.120119

Rogerson, M., Rohling, E. J., Bigg, G. R., & Ramirez, J. (2012). Paleoceanography of the Atlantic-Mediterranean exchange: Overview and first quantitative assessment of climatic forcing. *Reviews of Geophysics*, *50*(2). https://doi.org/10.1029/2011RG000376

Rohling, E. J. (1994). Review and new aspects concerning the formation of eastern Mediterranean sapropels. *Marine Geology*, *122*(1–2), 1–28. https://doi.org/10.1016/0025-3227(94)90202-X

Rohling, E. J., Marino, G., & Grant, K. M. (2015). Mediterranean climate and oceanography, and the periodic development of anoxic events (sapropels). *Earth-Science Reviews*, *143*, 62–97. https://doi.org/10.1016/j.earscirev.2015.01.008

Rossignol-Strick, M. (1983). African monsoons, an immediate climate response to orbital insolation. *Nature*, *304*(5921), 46–49. https://doi.org/10.1038/304046a0

Rutberg, R. L., Hemming, S. R., & Goldstein, S. L. (2000). Reduced North Atlantic deep water flux to the glacial southern ocean inferred from neodymium isotope ratios. *Nature*, *405*(6789), 935–938. https://doi.org/10.1038/35016049

Schacht, U., Wallmann, K., & Kutterolf, S. (2010). The influence of volcanic ash alteration on the REE composition of marine pore waters. *Journal of Geochemical Exploration*, *106*(1–3), 176–187. https://doi.org/10.1016/j.gexplo.2010.02.006

Schacht, U., Wallmann, K., Kutterolf, S., & Schmidt, M. (2008). Volcanogenic sediment–seawater interactions and the geochemistry of pore waters. *Chemical Geology*, *249*(3–4), 321–338. https://doi.org/10.1016/j.chemgeo.2008.01.026

Schmiedl, G., Kuhnt, T., Ehrmann, W., Emeis, K. C., Hamann, Y., Kotthoff, U., et al. (2010). Climatic forcing of eastern Mediterranean deep-water formation and benthic ecosystems during the past 22 000 years. *Quaternary Science Reviews*, *29*(23–24), 3006–3020. https://doi.org/10.1016/j.quascirev.2010.07.002

Scrivner, A. E., Vance, D., & Rohling, E. J. (2004). New neodymium isotope data quantify Nile involvement in Mediterranean anoxic episodes. *Geology*, *32*(7), 565–568. https://doi.org/10.1130/G20419.1

Shields, G. A., & Webb, G. E. (2004). Has the REE composition of seawater changed over geological time? *Chemical Geology*, *204*(2004), 103–107. https://doi.org/10.1016/j.chemgeo.2003.09.010

Sholkovitz, E. R. (1989). Artifacts associated with the chemical leaching of sediments for rare-earth elements. *Chemical Geology*, *77*(1), 47–51. https://doi.org/10.1016/0009-2541(89)90014-4

Siani, G., Magny, M., Paterne, M., Debret, M., & Fontugne, M. (2013). Paleohydrology reconstruction and Holocene climate variability in the South Adriatic Sea. *Climate of the Past*, *9*(1), 499–515. https://doi.org/10.5194/cp-9-499-2013

Siani, G., Paterne, M., Arnold, M., Bard, E., Métivier, B., Tisnerat, N., & Bassinot, F. (2000). Radiocarbon reservoir ages in the Mediterranean Sea and black sea. *Radiocarbon*, *42*(2), 271–280. https://doi.org/10.1017/S0033822200059075

Siani, G., Paterne, M., & Colin, C. (2010). Late glacial to Holocene planktic foraminifera bioevents and climatic record in the South Adriatic Sea. *Journal of Quaternary Science*, *25*(5), 808–821. https://doi.org/10.1002/jqs.1360

Siani, G., Paterne, M., Michel, E., Sulpizio, R., Sbrana, A., Arnold, M., & Haddad, G. (2001). Mediterranean Sea surface radiocarbon reservoir age changes since the last glacial maximum. *Science*, *294*(5548), 1917–1920. https://doi.org/10.1126/science.1063649

Siani, G., Sulpizio, R., Paterne, M., & Sbrana, A. (2004). Tephrostratigraphy study for the last 18,000 14C years in a deep-sea sediment sequence for the South Adriatic. *Quaternary Science Reviews*, *23*(23–24), 2485–2500. https://doi.org/10.1016/j.quascirev.2004.06.004

Siddall, M., Khatiwala, S., van de Flierdt, T., Jones, K., Goldstein, S. L., Hemming, S., & Anderson, R. F. (2008). Towards explaining the Nd paradox using reversible scavenging in an ocean general circulation model. *Earth and Planetary Science Letters*, *274*(3–4), 448–461. https://doi.org/10.1016/j.epsl.2008.07.044

Skinner, L. C., Sadekov, A., Brandon, M., Greaves, M., Plancherel, Y., de La Fuente, M., et al. (2019). Rare Earth Elements in early-diagenetic foraminifer 'coatings': Pore-water controls and potential palaeoceanographic applications. *Geochimica et Cosmochimica Acta*, *245*, 118–132. https://doi.org/10.1016/j.gca.2018.10.027

Spivack, A. J., & Staudigel, H. (1994). Low-temperature alteration of the upper oceanic crust and the alkalinity budget of seawater. *Chemical Geology*, *115*(3–4), 239–247. https://doi.org/10.1016/0009-2541(94)90189-9

Stoll, H. M., Vance, D., & Arevalos, A. (2007). Records of the Nd isotope composition of seawater from the Bay of Bengal: Implications for the impact of Northern Hemisphere cooling on ITCZ movement. *Earth and Planetary Science Letters*, *255*(1–2), 213–228. https://doi.org/10.1016/j.epsl.2006.12.016

Tachikawa, K., Arsouze, T., Bayon, G., Bory, A., Colin, C., Dutay, J. C., et al. (2017). The large-scale evolution of neodymium isotopic composition in the global modern and Holocene ocean revealed from seawater and archive data. *Chemical Geology*, *457*, 131–148. https://doi.org/10.1016/j.chemgeo.2017.03.018

Tachikawa, K., Athias, V., & Jeandel, C. (2003). Neodymium budget in the modern ocean and paleo-oceanographic implications. *Journal of Geophysical Research*, *108*(C8). https://doi.org/10.1029/1999JC000285

Tachikawa, K., Jeandel, C., & Roy-Barman, M. (1999). A new approach to the Nd residence time in the ocean: The role of atmospheric inputs. *Earth and Planetary Science Letters*, *170*(4), 433–446. https://doi.org/10.1016/S0012-821X(99)00127-2

Tachikawa, K., Piotrowski, A. M., & Bayon, G. (2014). Neodymium associated with foraminiferal carbonate as a recorder of seawater isotopic signatures. *Quaternary Science Reviews*, *88*, 1–13. https://doi.org/10.1016/j.quascirev.2013.12.027

Tachikawa, K., Roy-Barman, M., Michard, A., Thouron, D., Yeghicheyan, D., & Jeandel, C. (2004). Neodymium isotopes in the Mediterranean Sea: Comparison between seawater and sediment signals. *Geochimica et Cosmochimica Acta*, *68*(14), 3095–3106. https://doi.org/10.1016/j.gca.2004.01.024

Tachikawa, K., Toyofuku, T., Basile-Doelsch, I., & Delhaye, T. (2013). Microscale neodymium distribution in sedimentary planktonic foraminiferal tests and associated mineral phases. *Geochimica et Cosmochimica Acta*, *100*, 11–23. https://doi.org/10.1016/j.gca.2012.10.010

Tanaka, T., Togashi, S., Kamioka, H., Amakawa, H., Kagami, H., Hamamoto, T., et al. (2000). JNdi-1: A neodymium isotopic reference in consistency with LaJolla neodymium. *Chemical Geology*, *168*(3–4), 279–281. https://doi.org/10.1016/S0009-2541(00)00198-4

Tharaud, M., Gardoll, S., Khelifi, O., Benedetti, M. F., & Sivry, Y. (2015). uFREASI: User-FRiendly Elemental dAta procesSIng. A free and easy-to-use tool for elemental data treatment. *Microchemical Journal*, *121*, 32–40. https://doi.org/10.1016/j.microc.2015.01.011

Tomlinson, E. L., Smith, V. C., Albert, P. G., Aydar, E., Civetta, L., Cioni, R., et al. (2015). The major and trace element glass compositions of the productive mediterranean volcanic sources: Tools for correlating distal tephra layers in and around Europe. *Quaternary Science Reviews*, *118*, 48–66. https://doi.org/10.1016/j.quascirev.2014.10.028

Totaro, F., Insinga, D. D., Lirer, F., Margaritelli, G., i Caparrós, A. C., de la Fuente, M., & Petrosino, P. (2022). The Late Pleistocene to Holocene tephra record of ND14Q site (southern Adriatic Sea): Traceability and preservation of Neapolitan explosive products in the marine realm. *Journal of Volcanology and Geothermal Research*, *423*, 107461. https://doi.org/10.1016/j.jvolgeores.2021.107461

Uysal, I. T., & Golding, S. D. (2003). Rare earth element fractionation in authigenic illite–smectite from late permian clastic rocks, Bowen basin, Australia: Implications for physico-chemical environments of fluids during illitization. *Chemical Geology*, *193*(3–4), 167–179. https://doi.org/10.1016/S0009-2541(02)00324-8

Vance, D., Scrivner, A. E., Beney, P., Staubwasser, M., Henderson, G. M., & Slowey, N. C. (2004). The use of foraminifera as a record of the past neodymium isotope composition of seawater. *Paleoceanography*, *19*(2). https://doi.org/10.1029/2003PA000957

von Blanckenburg, F., & Igel, H. (1999). Lateral mixing and advection of reactive isotope tracers in ocean basins: Observations and mechanisms. *Earth and Planetary Science Letters*, *169*(1–2), 113–128. https://doi.org/10.1016/S0012-821X(99)00070-9

Weldeab, S., Emeis, K. C., Hemleben, C., & Siebel, W. (2002). Provenance of lithogenic surface sediments and pathways of riverine suspended matter in the eastern Mediterranean Sea: Evidence from 143Nd/144Nd and 87Sr/86Sr ratios. *Chemical Geology*, *186*(1–2), 139–149. https://doi.org/10.1016/S0009-2541(01)00415-6

Wilson, D. J., Piotrowski, A. M., Galy, A., & Clegg, J. A. (2013). Reactivity of neodymium carriers in deep sea sediments: Implications for boundary exchange and paleoceanography. *Geochimica et Cosmochimica Acta*, *109*, 197–221. https://doi.org/10.1016/j.gca.2013.01.042

Wu, J., Filippidi, A., Davies, G. R., & de Lange, G. J. (2018). Riverine supply to the eastern mediterranean during last interglacial sapropel S5 formation: A basin-wide perspective. *Chemical Geology*, *485*, 74–89. https://doi.org/10.1016/j.chemgeo.2018.03.037

Wu, J., Liu, C., Fürsich, F. T., Yang, T., & Yin, J. (2015). Foraminifera as environmental indicators and quantitative salinity reconstructions in the Pearl River estuary, Southern China. *Journal of Foraminiferal Research*, *45*(3), 205–219. https://doi.org/10.2113/gsjfr.45.3.205

Wu, J., Pahnke, K., Böning, P., Wu, L., Michard, A., & de Lange, G. J. (2019). Divergent Mediterranean seawater circulation during Holocene sapropel formation–Reconstructed using Nd isotopes in fish debris and foraminifera. *Earth and Planetary Science Letters*, *511*, 141–153. https://doi.org/10.1016/j.epsl.2019.01.036

Zhong, S., & Mucci, A. (1995). Partitioning of rare earth elements (REEs) between calcite and seawater solutions at 25 C and 1 atm, and high dissolved REE concentrations. *Geochimica et Cosmochimica Acta*, *59*(3), 443–453. https://doi.org/10.1016/0016-7037(94)00381-U

Ziegler, M., Tuenter, E., & Lourens, L. J. (2010). The precession phase of the boreal summer monsoon as viewed from the eastern Mediterranean (ODP Site 968). *Quaternary Science Reviews*, *29*(11–12), 1481–1490. https://doi.org/10.1016/j.quascirev.2010.03.011